Environmental Radiation in High Exposure Building Materials

Akbar Abbasi

Submitted to the

Institute of Graduate Studies and Research

in partial fulfillment of the requirements for the Degree of

Doctor of Philosophy

in

Physics

Eastern Mediterranean University

July 2013

Gazimağusa, North Cyprus

Approval of the Institute of Graduate Studies and Research

Prof. Dr. Elvan Yılmaz Director

I certify that this thesis satisfies the requirements as a thesis for the degree of Doctor of Philosophy in Physics.

Prof. Dr. Mustafa Halilsoy Chair,
Department of Physics

We certify that we have read this thesis and that in our opinion it is fully adequate in scope and quality as a thesis for the degree of Doctor of Philosophy in Physics.

Prof. Dr. Mustafa Halilsoy
Supervisor

Examining Committee

1. Prof. Dr. Uner Colak
2. Prof. Dr. Meral Eral
3. Prof. Dr. Ozay Gurtug
4. Prof. Dr. Mustafa Halilsoy
5. Assoc. Prof. Dr. Izzet Sakalli

ABSTRACT

In this thesis, we investigated the specific radioactivity concentrations of ^{226}Ra, ^{232}Th and ^{40}K in different types of commonly used granite stone samples collected from the Tehran city of Iran by means of a high-resolution HPGe gamma-spectroscopy system. The result of ^{232}Th, ^{226}Ra and ^{40}K are ranged from 18 to 178, 6 to 160 and 556 to1539 Bq kg^{-1}, respectively. The radium equivalent activities (Ra_{eq}) are lower than the limit of 370 Bq kg^{-1} set by NEA (Nuclear Energy Agency, OECD 1979) except in two samples. The internal hazard indexes have been found well below the acceptable limit in most of the samples. Five samples of investigated commercial granite stones do not satisfy the safety criterion illustrated by UNSCEAR (United Nations Scientific Committee on the Effects of Atomic Radiation, 1993). Applying dose criteria recently recommended by the EC [European Commission (1999)] for superficial materials, all investigated samples meet the exemption dose limit of 0.3 mSv y^{-1}.

Also in this thesis, health hazards from gamma radiation doses due to granite and radon concentration have been calculated. The dose rate of exposure from granite building materials on humans is obtained as a result of an external exposure from gamma-emitting radionuclides in the granites. Another mode of exposure is from the inhalation of the decay products of ^{222}Rn and ^{220}Rn. The radon exhalation rates have also been studied and values were in the range of 0.32±0.01 to 7.86±1.65 Bq m^{-2} h^{-1}. For two models of standard living rooms (5.0 m×4.0 m area; 2.8 m), the radon concentration (C_i) and the absorbed dose (D) rates were calculated and the results were found to be 10.64–29.32 Bq m^{-3}, 3.84–68.02 nGy h^{-1} and 0.02–0.33 mSv y^{-1} for

Model 1, 10.07–15.38 Bq m^{-3} and 2.29–39.99 nGy h^{-1} for Model 2, respectively. According to our estimations, mechanical ventilation systems ($\lambda_v = 0.5\, h^{-1}$) in a room all granite samples would produce radon concentration of <100 Bq m^{-3}.

Finally, radon exhalation rates and radon concentrations in selected granite stones were measured by means of a gamma-spectroscopy system (passive method) and an AlphaGUARD (active method). The radon exhalation rates measured by the passive and active methods were compared and the results of this study were similar, with the active method being 22 % higher than the passive method.

Keywords: Radioactivity, Internal Hazard, Radiation Dose, Radon Exhalation, Passive Method, Active Method.

ÖZ

Bu tezde yüksek çözünürlüklü HPGe gama spektroskopi sistemi kullanarak Tahran/IRAN daki farkli tür granit taşlarının ^{226}Ra, ^{232}Th ve ^{40}K kaynaklı radyoaktivite yoğunlukları incelenmiştir. Sırası ile; ^{232}Th, ^{226}Ra ve ^{40}K için 18 - 179, 6 – 160 ve 556 – 1539 Bq/kg sonuçlari elde edilmiştir. İki örnek dışında (1979) OECD Nükleer Enerji Ajansının Koyduğu sınır değer olan 370 Bq/kg altinda değerler bulunmuştur. Pekçok örnekde tehlike (risk) indisleri kabul edilir limitlerde elde edilmiştir. İncelenen ticari granit taşlarından 5 örnek, UNSCLEAR (1993, Atomik Radyasyonun etkileri üzerine Birleşmiş Milletler Bilimsel Komitesi) in koyduğu güvenlik şartlarını sağlamaktadır. 1999 yılında Avrupa Komisyonunun önerdiği ölçek kuralları ışığında yüzeysel maddeler incelenmiş ve 0.3 mSv/yıl sınır değeri aşılmamıştır.

Granitteki gama ışınlarından ve radon yoğunluklarından oluşan sağlık riskleri de hesaplanmıştır. Granit yapı materyallerinin insana ışınlanma doz hızı, granitteki gama ışını yayan radyonukleitlerin diş işinlamasi sorunu oluşmaktadir.

Diger bir maruz kalma ise ^{222}Rn ve ^{226}Ra nin bozunma ürünlerinin solunumla alınmasıdır. Radon yayma oranları 0.32 ±0.01 – 7.86±1.15 $Bq/m^2 \cdot sa$ bulunmuştur. 5×4 (alan m^2)× 2.8 m'li standart odasında iki model için radon yoğunluğu (C_i) ve sogurulan doz (D) hesap edilmiştir. Hesaplanmış sonuçlar Model 1`in: 10.64 -29.32 $Bq/m^3$ , 3.84 – 68.02 nGy/sa ve 0.02 – 0.33 mSv/yıl. Model 2`in: 10.07 – 15.38 Bq/m^3 , ve 2.29 – 39.99 nGy/sa bulunmuştur.

Öngörümüze göre, mekanik havalandırma sistemli ($\lambda_v = 0.5\ /sa$) odada granit örneklerinin ürettiği radon yoğunluğu 100 Bq/m^3 altındadır.

Sonuç olarak, seçilmiş granit taşların radon çıkış oranı ve yoğunlukları gama Spektroskopi sistemi ile (pasif yöntem) ve AlphaGUARD (aktif yöntem) ile ölçülmüştür. Bu iki yöntemde sonuçlar kıyaslanmış olup benzer sonuçlar yanında aktif yöntemde 22% daha yüksek veriler tesbit edilmiştir.

Anahtar kelimeler: Radyoaktivite, Konutlardaki Tehlike, Işınım Dozları, Radon Çıkışı, Pasif ve Aktif Yöntemler.

To My Family

ACKNOWLEDGMENTS

I would like to express my deep sincere feelings to my supervisor Prof. Dr. Mustafa Halilsoy for his continuous support and guidance in the preparation of this project. Without his invaluable supervision, all my efforts could have been short-sighted. I am deeply thankful to Prof. Dr. Ozay Gurtug for his meticulous effort in teaching me numerous basic knowledge concepts.

I am also grateful to Prof. Dr Thomas Hinton for his help during my thesis. I would like to thank faculty member of Physics Department Assoc. Prof. Dr. Izzet Sakalli, Prof. Dr. Omar Mustafa and Assist. Prof. Dr. Habib Mazharimousavi. Besides, a number of my friends had always been around to support me. I would like to thank them as well.

I would like to thank also Prof. Dr. Majid Hashemipour and Prof. Dr. Osman Yilmaz Vice-Rector of the Eastern Mediterranean University; they provided me unflinching encouragement and support in various ways. Finally, I would like to express my gratitude to my wife and my family for their morale supports.

TABLE OF CONTENTS

LIST OF TABLES

LIST OF FIGURES

Chapter 1

INTRODUCTION

1.1 Source of Environmental Radiation

The environmental radiation sources are two types' natural source and man-made radioactive radionuclides. In natural causes exposures occurring due to radionuclides are discovered in the earth structure. The other radionuclides are produced in the atmosphere by space radiation. Man-made radionuclides have gone into the environment due to human activities like for example medical purposes that use radionuclides to diagnosis and therapy the body. Other man made causes are power plant reactors that use radioactive uranium and thorium as fuel. We are ceaselessly exposed to radiation by sources external and internal our bodies. The terrestrial radiation and space radiation are external sources. Internal radiation are radionuclides that enter human bodies with the food, drinking water and air by ingest and exhale.

1.1.1 Terrestrial Radiation Source

Radiation that has the origin from Earth is named terrestrial radiation. Primordial radionuclides (radionuclides that were present when the Earth created about 4.5×10^9 years ago) are detected in the earth. This radionuclides are mixed in stones, rocks even water. These radionuclides are released into water and air from soil and rocks. Also uranium mining and fuel cycle that causes are redistributed terrestrial radionuclides. The important primordial radionuclides include the series ^{238}U, ^{232}Th

and their decay products, as well as ^{40}K and ^{87}Rb. previously, one of the human activities that contributed to terrestrial radiation was the nuclear weapons production.

The Chernobyl Accident in 1986, which was an explosion at power reactor, is also another source to increasing background radiation in the world. However, almost all radionuclides that were produced in this mentioned were decayed except ^{137}Cs and ^{90}Sr radionuclides.

1.1.2 Cosmic Radiation

The space radiation and particles come into the Earth's atmosphere from space. Their source are the Earth's radiation belts and the sun or as far away as beyond the boundaries of the solar system. There are two types of radiation: I) galactic cosmic rays (GCR), II) radiation emanating from the Sun. The particle and radiation energy ranges vary spaciously.

The biological effect is a combination of the primary particles and the secondary particles. Radiation with beyond solar system sources can transport through Earth's atmosphere, because they have high range energy. This radiation can generate additional fall radiation. They are creating either radionuclide in the atmosphere or secondary fall particles. Almost secondary particles can reach the atmosphere and Earth's surface at high altitudes where the Earth's atmosphere is delicate. The radionuclides are produced by cosmic radiation, named cosmogenic radionuclides. The important radionuclides are ^{3}H, ^{7}Be, ^{14}C and ^{22}Na.

1.1.3 Radiation of Radionuclides in the Body

In our daily life, the terrestrial and cosmogenic radionuclides are entered the human body through such as food, water and air. In this time the short-lived radionuclides are significant since the short-lived radionuclides decay away quickly in body and the long-lived radionuclides are placed in body. These radionuclides are decayed more slowly and collected in specific body tissues for example radon in lung. The terrestrial source radionuclides are the most important radionuclides that enter the human bodies. The radon gases are important ones (and their decay chain radionuclides) that we continuously inhale. Other radionuclides in the body, is as well as ^{40}K. Surface drinking water have very low levels of terrestrial radionuclides however, the ^{226}Ra, ^{228}Ra, and ^{238}U are mixed in ground water. These radionuclides may be higher in some areas of the world than in others places.

1.2 Dose from Nuclear Radiation

The nuclear radiation dose from exposure to radiation sources are received by human body via two ways. The outside and inside of body: the outside is for example external radiation from ^{238}U in concrete used to build materials in dwelling and the inside the body is internal radiation from radioactive ^{40}K absorbed by the cells when one eats food. Another radiation source is medical exposures. The main effective dose units is Sievert (Sv), however, we are using (mSv) and (μSv) as dose units. Sievert is the dose equivalent that equalizes biological effects from different types and energy of radiation. Another absorbed dose unit is the gray (Gy) is the quantity of energy (J) that deposited in a unit mass (kg) in human tissue or other material.

According to UNSCEAR's (1982) reports, estimates the annual average effective dose equivalent per person in the world population is to be 3 mSv/y [1]. For this value, 2.4 mSv due to natural sources per year and 0.6 mSv attributed from man-made sources (Shown in Table 1.1).

1.3 Radon Decay Products

We know the radon as an inert gas with atomic number 86 and it has three natural isotopes with mass numbers 222, 220 and 219. These radioisotopes are respectively members of ^{238}U, ^{232}Th and ^{235}U series. Since the radon is in the gas form it can diffuse place to place, emanating from water, soil and socks and distributed in the air. The decay products of Rn-219 are difficult to detect in the environment and atmosphere, because its parent, U-235, composed of only 0.73 % by weight of natural uranium concentration. Three isotopes of radon are radioactive and decay by α-decay mode to daughter products.

According to UNSCEAR's 1982 reports, status of the relative indoor radon concentrations attributable to some sources [1]:

Building material	80 %
Outside air	10 %
Water (showers, etc.)	5 %
Natural gas	4 %
Liquefied petroleum gas	<1 %

In this research our purpose is to survey and measure the terrestrial radionuclides such as ^{232}Th, ^{238}U, ^{226}Ra, ^{40}K and ^{222}Rn gases in granite stones.

1.4 Radiation Exposure in Buildings Material

The gamma rays emitted from members of the uranium and thorium decay chains and ^{40}K are the most important sources of external radiation exposure in building materials [2]. It is an established fact that all the construction materials contain trace amounts of natural radioactivity [3]. Knowledge of radiation in building materials helps us to assess any possible radiological hazard to occupants of the dwelling [2]. The ^{238}U and ^{232}Th radionuclides concentration are in the Earth's crust in parts per million levels [4]. The potassium concentration is also present in the Earth's crust and 0.0118 % of the total amount of potassium is ^{40}K isotope.

As a result of uranium size and charge, the uranium atom does not tend to fit well into typical igneous rock-forming minerals (such as feldspars, quartz, micas, amphiboles, pyroxenes, olivine and titan magnetite) and tends to be concentrated in silicarich magmas such as rhyolites and granites [5]. Estimated levels of uranium, thorium and potassium concentrations in granite as building materials are 63, 8 and 1184 Bq kg^{-1}, respectively (NCRP 94) [6]. Indoor exposure to gamma rays, mainly determined by the construction materials, is inherently greater than outdoor exposure if materials from the earth are used for construction. The source geometry changes from half-space to a more surrounding configuration indoors. When the duration of occupancy is taken into account, indoor exposure becomes even more significant. This depends on the distribution and concentrations of the parent radium radionuclides in the bedrock and on the permeability of the soil. Certain

generalizations can be made about the radium concentrations in bedrocks of various types, but there are very large ranges within each type. In general, granites have relatively high radium content [7]. In the USA, only 37 % of the total effective dose equivalent is due to radon and thoron, whereas 48 % is attributed to medical diagnosis [8]. According to ref. [1], it was estimated that the inhalation of a short-lived decay product of radon (^{222}Rn) accounts on the average for about one-half of the effective dose equivalent from all natural sources of radiation and may sometimes lead to doses high enough to be a cause of concern for human health [9]. Radon gas is a radionuclide present in the earth's crust, which naturally originates from the disintegration of the radium (^{226}Ra) in the uranium (^{238}U) decay series. In many parts of the world, building materials containing radioactive elements are used for construction. As individuals spend 80 % of their time indoors, the internal and external radiation exposure due to building materials causes situations of prolonged exposure [10].

Radioactive radon gas has a half-life of 3.8 day that emanates from rocks and soils and tends to concentrate in enclosed spaces like underground mines or houses. Radon is a major contributor to the ionising radiation dose received by the general population. Recent studies on indoor radon and lung cancer in Europe, North America and Asia provide evidence that radon may cause a substantial number of lung cancer in the general population. Current estimates of the proportion of lung cancer attributable to radon range from 3 to 14 %, depending on the average radon concentration in the country concerned and the calculation methods [11]. It is well known that as a result of inhalation of ^{222}Rn, a daughter product of decay chain of ^{238}U and its daughter products' equivalent dose to entire lung is higher than the equivalent dose in other tissues [12]. Granite stones emit more radon (Rn) compared

with other types of construction materials because of the existence of relatively high uranium content [13]. Short-lived decay products of radon are the most important contributors to human exposure to ionizing radiation from natural sources. This contribution represents 50 % of the total annual human dose [14]. Indoor radon concentrations depend on many factors such as building materials, indoor–outdoor temperatures, relative humidity, air turbulence, air flow and ventilation rate as well as geological formations. It is important to evaluate the role and contribution of the different dwelling materials that can act as radon sources or radon absorber inside buildings for work and residence [15]. Generally, granite is believed to have a higher radon exhalation rate than other building material on average [16 – 19].

In total, the classification of natural radiation and man-made radiation we show the contribution of radiation exposure in Fig 1.1.

The sections of this thesis are as follows: in chapter 2, the theoretical basis is discussed. In this chapter we classify the types of radiation and their creation processes. In chapter 3, we briefly review the experimental methods and equipment that we use in measurements. The results and calculations of simulation program are discussed in the chapter 4. These results are including natural radioactivity in high exposer building material (granites), dose calculation, gamma radiation dose rate, radon concentration and comparing two methods to radon exhalation rate.

In chapter 5, we present the conclusion and discussion due to this research. Finally, we collected all references at the end of the thesis.

Table 1.1.The Annual Doses (in mSv) Due to Natural Sources of Radiation (UNSCEAR 2000)

Source	**Annual Average Dose (mSv)**	**Typical Range of Annual Dose (mSv)**
Inhalation (radon gas)	1.26	0.2-10
External terrestrial	0.48	0.3-1
Ingestion	0.29	0.2-1
Cosmic radiation	0.39	0.3-1
Total natural	2.42	1-13

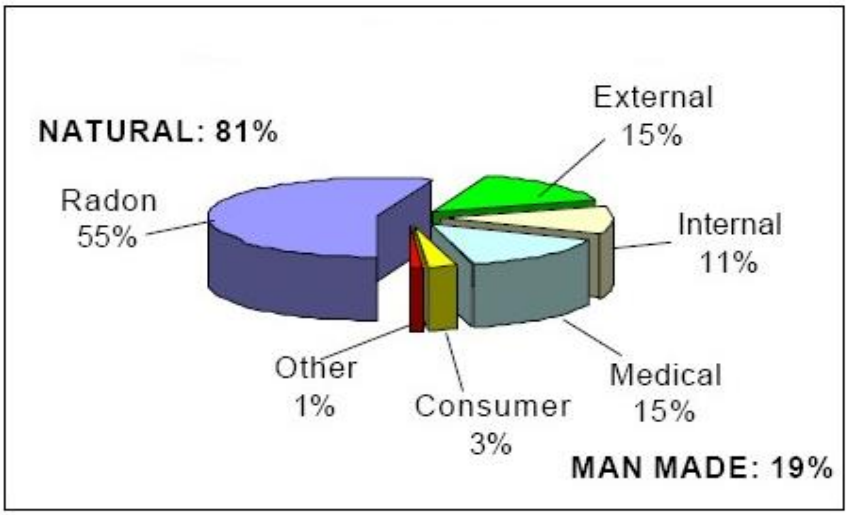

Figure 1.1.The Contribution of Radiation Exposure to the Public is from Natural and man-made sources of Radiation. (NCRP), 1998 [20]

From the forgoing analysis it can be emphasized that an alternative title for the present thesis could be expressed by "Natural Radioactivity and dose Calculation in Granite Samples used in Building Material".

In totally, the main result and outline of this research are following:

1- Two samples (G 4, G 17) cannot satisfy three of four safety indices.

2- According World Health Organization (WHO) indoor radon level is 100 Bq/m3, therefore:

   -For ventilation system rate (λ_v=0.5 h^{-1}): the radon concentration in all samples is less than this level (C_i< 100 Bq/m^3).

   -For poor ventilation system rate (λ_v=0.1 h^{-1}): only 7% of samples higher than reference level concentration.

3- In comparison two radon concentration measurement methods: The results are the same but variation value is 22% on averagely.

Chapter 2

THEORETICAL BASIS

In this section, we review briefly the classification of nuclear emission from radionuclides that exist in environment and our living place. Nuclear decays are described by their Q value and half-life. The lifetimes we consider vary over an extremely wide range of magnitudes. In terms of a=Log_{10}[$T_{1/2}$ (sec)] it is useful to keep in mind the values of a≈37 for the proton lifetime limit, a≈ 17 for the age of the universe (10 billion years), a≈ 5 for one day, a≈ −7 (100 nsec) for the typical time it takes to analyze a secondary beam from the cyclotron [21].

2.1 Decay Constant and Lifetimes

The decay of a radionuclide is described by the rate equation for the number of nuclei present at time t.

$$\frac{dN}{dt} = -\lambda N(t)$$

where N is the number of atoms, N(t) is the number of atom at time t and λ is the constant of decay or transition rate . The solution of this equation is the exponential decay law:

$$N(t) = N_0 e^{-\lambda t} \qquad (2.2)$$

The time at which the number is reduced by half is the half-life :($N_{T1/2}$= N_0/2)

$$T_{\frac{1}{2}} = \frac{ln2}{\lambda} = \frac{0.693}{\lambda} \tag{2.3}$$

The mean-lifetime τ is the average amount of time it takes to decay:

$$\tau = \frac{\int te^{-\lambda t}dt}{\int e^{-\lambda t}dt} = \frac{1}{\lambda} = \frac{T_{\frac{1}{2}}}{ln2} = \frac{T_{\frac{1}{2}}}{0.693} \tag{2.4}$$

A given initial state may decay to several final states. The total transition rate is:

$$\lambda = \sum_{f} \lambda_{i,f} \tag{2.5}$$

where $\lambda_{i,f}$ is the partial decay rate to the particular final state f. The branching fraction to this state is:

$$b(i \to f) = \frac{\lambda_{i,f}}{\lambda} \tag{2.6}$$

When the total lifetime and the branching fraction for a given decay are known, we can find the partial lifetime τ_p related to that specific decay channel by:

$$\tau_p = \frac{\tau}{b} \tag{2.7}$$

2.2 Production of a Radioisotope by Decay Series

The decay series is an important discussion in environmental radioactivity measurements. We have three radioactive chains in the environment such as ^{238}U,

^{235}U and ^{232}Th. The series begin by parent (1) with a decay constant λ_1 and decay produces a daughter (2) with decay constant λ_2 product a stable nuclei (3) and radiation r_2.

We suppose N_1, N_2 and N_3 are the respective numbers of radioactive nuclei present at any given time t. We can write:

$$\frac{dN_1}{dt} = -\lambda_1 N_1$$

$$\frac{dN_2}{dt} = \lambda_1 N_1 - \lambda_2 N_2$$

$$\frac{dN_3}{dt} = \lambda_2 N_2 \tag{2.8}$$

If N_{01} is the original number of nuclei 1 present, we can write:

$$N_1 = N_{01} e^{-\lambda_1 t} \tag{2.9}$$

After substitution into Eq 2.8 and some calculation we obtain:

$$N_2 = \frac{N_{01}\lambda_1}{\lambda_2 - \lambda_1}\left(e^{-\lambda_1 t} - e^{-\lambda_2 t}\right)$$

$$N_3 = \frac{N_{01}\lambda_1\lambda_2}{\lambda_2-\lambda_1}\left(\frac{1-e^{-\lambda_1 t}}{\lambda_1} - \frac{1-e^{-\lambda_2 t}}{\lambda_2}\right) \tag{2.10}$$

If $\lambda_1 > \lambda_2$ after a long time t ($\gg 1/\lambda_1$):

$$e^{-\lambda_1 t} \ll e^{-\lambda_2 t}$$

$$N_2 \approx \frac{N_{01}\lambda_1}{\lambda_1 - \lambda_2}\left(e^{-\lambda_2 t}\right) \tag{2.11}$$

Therefore, the decay of daughter after long time is determined only by its own half-life.

If the parent is long-lived ($\lambda_1 < \lambda_2$), after a long time as mentioned in Eq 2.11:

$$N_2 \approx \frac{N_{01}\lambda_1}{\lambda_2 - \lambda_1}\left(e^{-\lambda_1 t}\right) \tag{2.12}$$

$$\frac{N_2\lambda_2}{N_1\lambda_1} \approx \frac{\lambda_2}{\lambda_2 - \lambda_1} \tag{2.13}$$

This state is called transient equilibrium between parent and daughter radionuclide.

The secular equilibrium is obtained when $\lambda 1 \ll \lambda 2$, this condition exists between Ra-226 and Rn-222 radionuclides.

2.3 Alpha Decay

The theoretical side for alpha decay was developed by George Gamow and others in 1930s. One postulates an alpha particle moving in the potential well of an attractive strong interaction. Decay of alpha particle occurs when a parent nucleus (A, Z) with atomic mass number A and nuclear charge number Z spontaneously emits an alpha particle leaving a residual (daughter) nucleus (A − 4, Z − 2):

$$^{A}_{Z}X \rightarrow ^{A-4}_{Z-2}Y + ^{4}_{2}He \tag{2.14}$$

Alpha decay usually occurs from the nuclear ground state, but decay from excited states may also is possible. The alpha decay of a given parent nucleus often leads to daughter nuclei that are themselves alpha or beta radioactive, thus giving rise to a disintegration radioactive series.

According to conservation of energy and momentum we can write two equations in alpha decay procedure:

$$M_p c^2 = M_D c^2 + T_D + M_\alpha c^2 + T_\alpha$$

$$0 = P_D + P_\alpha \tag{2.15}$$

where M_p is the nuclear mass of parent ; M_D nuclear mass of daughter ; M_α nuclear mass of alpha particle; T_D recoil kinetic energy; T_α kinetic energy of alpha particle; P_D momentum of parent; P_α momentum of alpha particle.

The decay energy for alpha particle (Q_α):

$$Q_\alpha = \frac{M_D + M_\alpha}{M_D} T_\alpha \approx \frac{A}{A-4} T_\alpha \tag{2.16}$$

and the Q_α is given in terms of binding energies B by:

$$Q_\alpha = B(N-2, Z-2) + B(2,2) - B(N,Z) \tag{2.17}$$

where B(2, 2) = 28.296 MeV.

2.4 Beta Decay

In beta decay procedure the neutron/proton make change to a proton/neutron, an electron/positron, and an electron antineutrino/neutrino:

$$n \rightarrow p + e^- + \bar{\nu} \quad \text{and} \quad p \rightarrow n + e^+ + \nu$$

Nuclei are composed of protons and neutrons bound together by the strong interaction. In the beta decay of nuclei, a given initial nuclear state A_iZ_i is converted into the ground state or an excited state of the final nucleus A_fZ_f , where $Z_f = Z_{i\pm1}$. The transition rate for nuclear beta decay is determined by the Q_β value or energy release and the structure of the initial and final nuclear states.

Beta decays with the fastest rates occur when the leptons carry away ℓ=0 angular momentum and are referred to as "allowed" transitions. Decays with ℓ >0 for the leptons are referred to as "forbidden" transitions. The dependence upon the energy release can usually be calculated to a precision of about 0.1 percent, and beta decay thus provides a precise test of the strength of the weak interaction, as well as of the internal structure of particles and nuclei. In the limit when Z is small and Q_β is large, the transition rate for "allowed" beta transitions is proportional to Q_β^5 [22].

Beta minus, β^-, decay involves the emission of an electron and electron antineutrino:

$$ {}^{A}_{Z}X \rightarrow {}_{Z+1}{}^{A}Y + e^- + \bar{\upsilon} \tag{2.18} $$

The Q value for β^- decay is given in terms of nuclear masses M and nuclear binding energies B.E by:

$$ \begin{aligned} Q(\beta^-) &= [M(A,Z) - M_{-1}(A,Z+1) - m_e]c^2 \\ &= [M(A,Z) - M(A,Z+1)]c^2 \\ &= B(N,Z+1) - B(N,Z) + \delta_{nH} \end{aligned} \tag{2.19} $$

where $m_e c^2 = 0.511\ MeV$,

$$M_{-1}(A, Z+1) = M(A, Z+1) - m_e \tag{2.20}$$

is the mass of the final nucleus with one electron missing, and

$$\delta_{nH} = \Delta_n c^2 - \Delta_H c^2 = 0.782\ MeV \tag{2.21}$$

comes from the mass difference between the neutron and the Hydrogen atom. In these expressions we assume that the mass of the neutrino is zero and we ignore the electronic binding energy.

Beta plus, β^+, decay involves emission of $e^+$and e^-neutrino:

$$^A_Z X \rightarrow {}^A_{Z-1} Y + e^+ + \nu \tag{2.22}$$

The Q value for β^+ decay:

$$\begin{aligned} Q(\beta^+) &= [M(A,Z) - M_{+1}(A, Z-1) - m_e]c^2 \\ &= [M(A,Z) - M(A, Z-1) - 2m_e]c^2 \\ &= B(N, Z-1) - B(N,Z) - 2m_e c^2 - \delta_{nH} \end{aligned} \tag{2.23}$$

Where

$$M_{+1}(A, Z-1) = M(A, Z-1) + m_e \tag{2.24}$$

is the mass of the final nucleus with one extra electron.

Another form of beta decay that competes with β^+ decay is electron capture (EC) in which one of the atomic electrons is captured by the nucleus and a neutrino is emitted:

$$e^- + {}^{A}_{Z}X \rightarrow {}^{A}_{Z-1}Y + \upsilon \qquad (2.25)$$

The Q value for electron capture decay is given by:

$$Q(EC) = [M(A,Z) - M(A,Z-1)]c^2$$
$$= B(A,Z-1) - B(A,Z) - \delta_{nH} \qquad (2.26)$$

The energy released in β^- or β^+ decay is shared between the recoiling nucleus, the electron and the neutrino. Usually only the electron or positron is detected, and it has a range of kinetic energies ranging from zero up to E_{max} (the end-point energy), assuming that the mass of the neutrino is zero. (see figure 2.1).

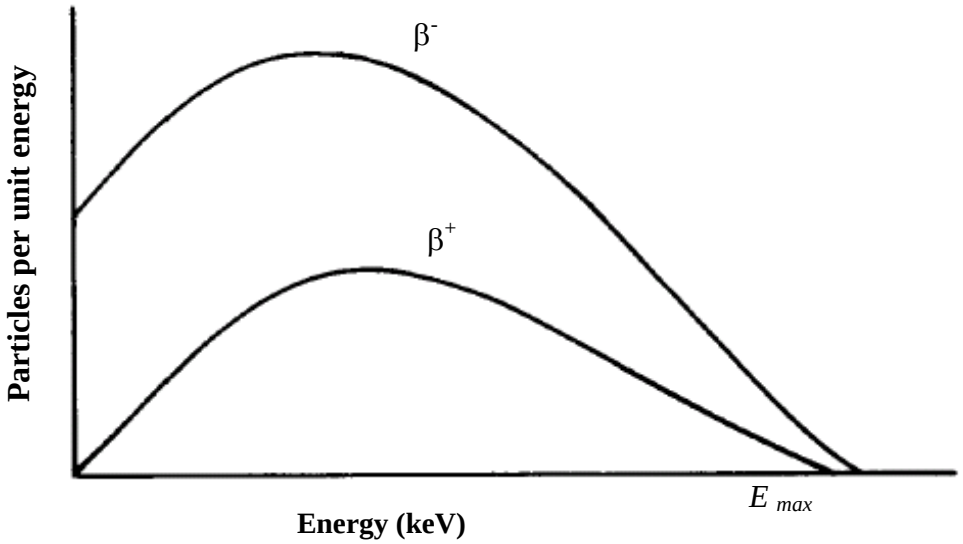

Figure 2.1 A typical beta energy spectrum [22]

2.5 Gamma Decay

In gamma decay, a nucleus goes from an excited state to a lower state and the energy difference between the two states is released in the form of a photon. Gamma decay is represented by:

$$ {}^{A}_{Z}X^{*} \rightarrow {}^{A}_{Z}X + \gamma \tag{2.27} $$

For an electromagnetic transition from an initial nuclear state i (where the nucleus is at rest) to nuclear state f, the momentum of the nucleus in state f (after the transition) and the emitted gamma ray are equal and opposite. The nucleus recoils with a kinetic energy:

$$ T_f = \frac{(\Delta E)^2}{2m_f c^2} \tag{2.28} $$

and the gamma ray has an energy:

$$ E_\gamma = \Delta E - T_f \tag{2.29} $$

Here ΔE=$E_f - E_i$ is the rest-mass energy difference between initial and final nuclear states. T_f is much smaller than ΔE and thus to a good approximation E_γ = ΔE. The electromagnetic transition between them can take place only if the emitted gamma ray carries away an amount of angular momentum $\vec{l}$ such that $\vec{J}_f = \vec{J}_i + \vec{l}$ which means that:

$$ \left|\vec{J}_i - \vec{J}_f\right| \leq l \leq \left|\vec{J}_i + \vec{J}_f\right| \tag{2.30} $$

Since the photon has an intrinsic spin of one, transitions with ℓ=0 are forbidden, and hence gamma transitions with $J_i = 0 \rightarrow J_f = 0$ are not allowed. A specific ℓ value

determines the multipolarity of the gamma radiation; ℓ=1 is called dipole, ℓ=2 is called quadruple, etc. In addition, when states can be labeled with a definite parity π_i=±1 and π_f=±1,the transitions between them are restricted to the "electric" type of radiation when $\pi_i\pi_f\,(-1)^l$ is even and the "magnetic" type of radiation when $\pi_i\pi_f\,(-1)^l$ is odd. In gamma decay, energy is mono peak as we see figure (2.2).

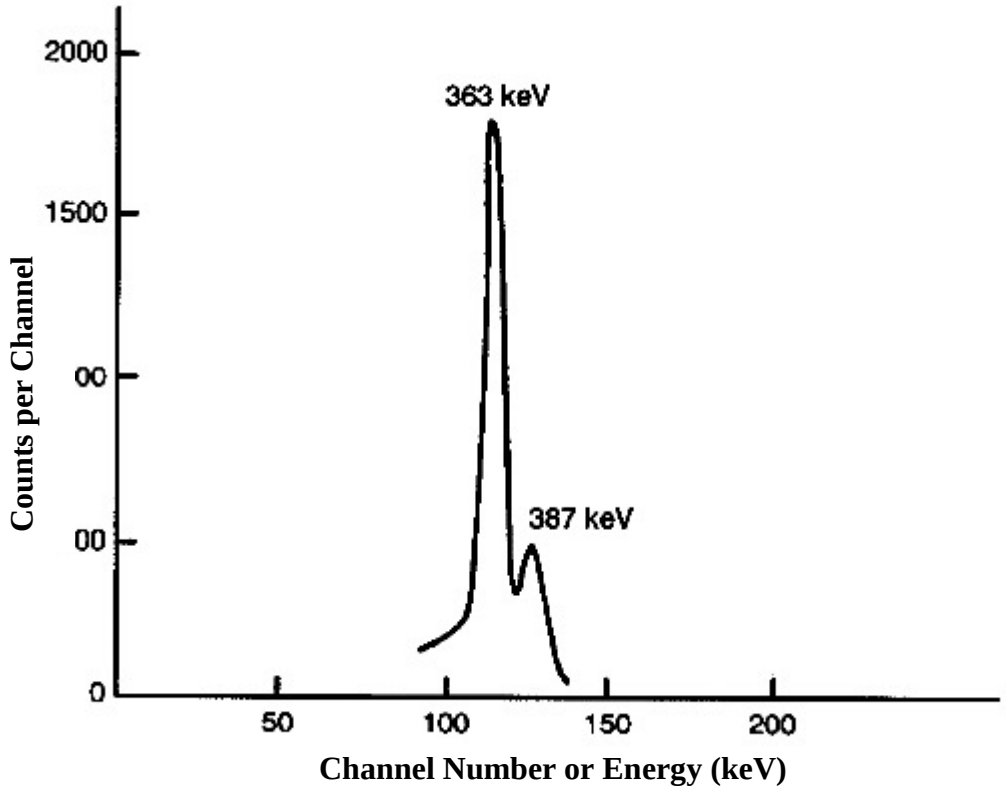

Figure 2.2. The internal conversion gamma spectrum of ^{113}Sn [23]

2.6 Material and Particle Interaction

The material is containing atoms, when particle moving through a material exerts Coulomb forces on many atoms simultaneously. Each interaction with atoms has its own probability for occurrence and for a certain energy loss. It is impossible to

calculate the energy loss by studying individual collisions. Instead, an average energy loss is calculated per unit distance traveled. The calculation is slightly different for electrons or positrons than for heavier charged particles like *p*, *d*, and α, for the following reason. If the incoming charged particle is an electron or a positron, it may collide with an atomic electron and lose all its energy in a single collision because the collision involves two particles of the same mass.

2.6.1 Stopping Power for p, d, t, α

Assuming that all the atoms and their atomic electrons act independently, and considering only energy lost to excitation and ionization, the average energy loss per unit distance traveled by the particle is given by:

$$\frac{dE}{dx}\left(\frac{MeV}{m}\right) = 4\pi r_0^2 z^2 \frac{mc^2}{\beta^2} N.Z\left[ln\left(\frac{2mc^2}{I}.\beta^2\gamma^2\right) - \beta^2\right] \qquad (2.31)$$

where $r_0 = \frac{e^2}{mc^2} = 2.818 \times 10^{-15} m$ $(electron\ radius\ in\ classic)$,

$4\pi r_0^2 = 9.98 \times 10^{-29}\ m^2$,

$mc^2 = 511\ keV$ $(rest\ mass\ energy\ of\ electron)$,

$\gamma = \frac{1}{\sqrt{1-\beta^2}}$ $\quad and \quad$ $\beta = \frac{v}{c}$

$N = Number\ of\ atoms\ per\ m^3$ $\quad or \quad$ $(\rho.\frac{N_A}{A})$

$Z = Atomic\ number\ of\ the\ target\ material$

$z = Charge\ of\ the\ incident\ particle$

$(z = 1\ for\ e-, e+, p, d; and\ z = 2\ for\ \alpha),$

$I = mean\ excitation\ potential\ of\ the\ material$

An approximate equation for I, which gives good results for Z > 12, is

$$I(eV) = (9.76 + 58.8\, Z^{-1.19})Z \qquad (2.32)$$

2.6.2 Stopping Power for Electrons and Positrons

Interactions between electrons and positrons with material are represented in Eq. 2.33 and 2.34, respectively. Their disagreement is due to the second term of equation, which is always much smaller than the logarithmic term. For an electron and positron with the same kinetic energy, Eqs. 2.33 and 2.34 provide results that are different by about 10 percent or less. For electron interaction:

$$\frac{dE}{dx}\left(\frac{MeV}{m}\right) = 4\pi r_0^2 z^2 \frac{mc^2}{\beta^2} N.Z \left\{ ln\left(\frac{\beta\gamma\sqrt{\gamma-1}}{I}.mc^2\right) + \right.$$
$$\left. + \frac{1}{2\gamma^2}\left[\frac{(\gamma-1)^2}{8} + 1 - (\gamma^2 + 2\gamma - 1)ln2\right]\right\} \qquad (2.33)$$

and for positron interaction:

$$\frac{dE}{dx}\left(\frac{MeV}{m}\right) = 4\pi r_0^2 z^2 \frac{mc^2}{\beta^2} N.Z \left\{ ln\left(\frac{\beta\gamma\sqrt{\gamma-1}}{I}.mc^2\right) - \right.$$
$$\left. - \frac{\beta^2}{24}\left[23 + \frac{14}{\gamma+1} + \frac{10}{(\gamma+1)^2} + \frac{4}{(\gamma+1)^3}\right] + \frac{ln2}{2}\right\} \qquad (2.34)$$

2.7 Interaction of γ- Photon with Matter

Photons are electromagnetic radiation which travels with the speed of light (c), zero rest mass and without charge. The gamma-ray interactions are three important absorption processes including: photoelectric effect (P.E), Compton scattering (C.S), and pair production (P.P).

2.7.1 Photoelectric Effect

In the photoelectric effect, a photon disappears and one of the atomic electrons is ejected as a free electron. The equation of kinetic energy and the photoelectric coefficient are written as:

$$T = E_\gamma - B_e \tag{2.35}$$

where E_γ is energy of the photon, T is kinetic energy of the electron and B_e is binding energy of the electron.

$$\tau(m^{-1}) = aN.\frac{Z^n}{E_\gamma^m}[1 - \mathcal{O}(Z)] \tag{2.36}$$

Here τ is the probability of interaction of photon by photoelectric effect in unit distance of the first order in Z [23].

Figure 2.3 shows the photoelectric effect importance with the other interactions as E_γ and Z change.

2.7.2 Compton Scattering

The Compton scattering occur between a photon and a free electron. The photon energy is reduced by a certain amount that is given to the electron. Hence, according conservation of energy:

$$T = E_\gamma - E_{\gamma'} \tag{2.37}$$

where T is kinetic electron energy, E_γ is initially photon energy and $E_{\gamma'}$ is the scattered photon energy.

Whereas, we can use the conservation of momentum equations to calculate the energy of the scattering in θ angle:

$$E_{\gamma'} = \frac{E_\gamma}{1 + (1 - cos\vartheta).E_\gamma/mc^2} \tag{2.38}$$

Figure 2.3 shows the Compton scattering importance with the other interactions as E_γ and Z change.

2.7.3 Pair Production

The Pair Production action is an interaction between a photon and a nucleon. In this interaction the photon disappears and an e^- - e^+ pair appears after that two 0.511-MeV photons are produced when the positron annihilates. Although the nucleus does not undergo any change as a result of this interaction, its presence is necessary for pair production to occur. A photon ($E \geq 1.022\ MeV$) will not disappear in empty space by producing an electron-positron pair.

The available kinetic energy is:

$$T_{e^-} = T_{e^+} = \frac{1}{2} + \left(E_\gamma - 1.022\ MeV\right) \tag{2.39}$$

The probability for pair production to happen, called the pair production coefficient or cross section is a complicated function of E, and Z:

$$\kappa(m^{-1}) = NZ^2 f\left(E_\gamma, Z\right) \tag{2.40}$$

where κ is the prospect for pair production to happen per unit distance and f(E,, Z) is a function that changes slightly with Z and increases with E_γ. Figure 2.3 shows the pair production importance with the other interactions as E_γ and Z change.

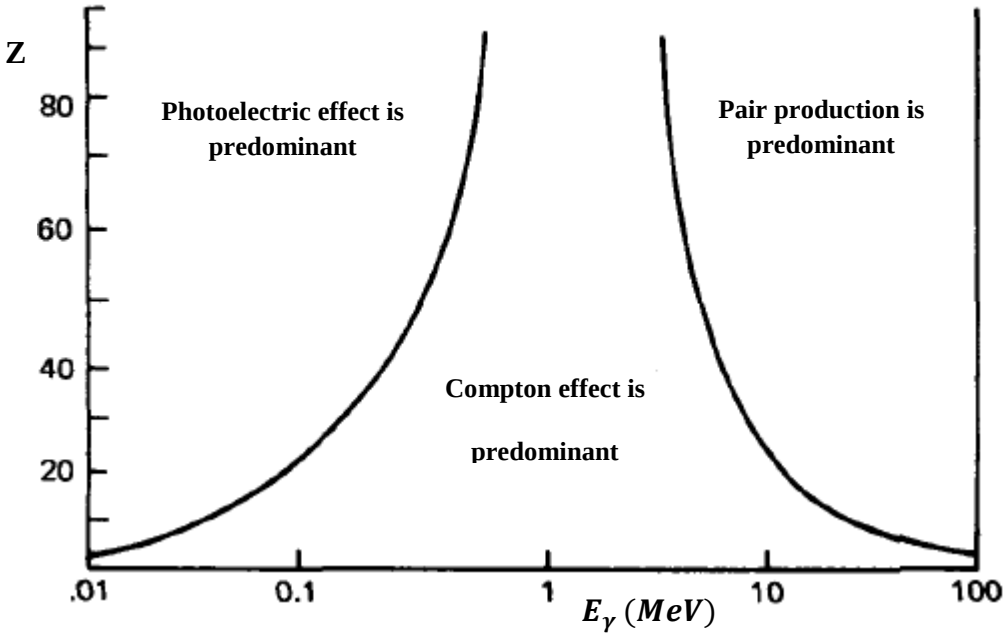

Figure 2.3.The Comparative Importance of the Three Major Gamma Interactions by matter [23]

2.8 The Statistical Error of Radiation Measurements

Radioactive decay is a random phenomenon that comply the Poisson distribution curve, according to standard deviation of the true mean m is $\sqrt{m}$. Suppose one performs only one measurement and the result is *n* counts. The best estimate of the true mean, as a result of this single measurement, is this number *n*. If one takes this to be the mean, its standard deviation will be $\sqrt{n}$.

Indeed, this is what is done in practice. The result of a single count *n* is reported as $\pm\sqrt{\boldsymbol{n}}$, which that:

1. The outcome *n* is considered the true mean.

2. The standard deviation is reported as the standard error of ***n.***

The relative standard error of the count *n* is

$$\frac{\sigma_n}{n} = \frac{1}{\sqrt{n}} \tag{2.41}$$

which shows that the relative error decreases if the number of counts obtained in the scaler increases. To increase the number *n,* one either counts for a long time or repeats the measurement many times and combines the results. Repetition of the measurement is preferable to one single long count because by performing the experiment many times, the reproducibility of the results is checked. Consider now a series of N counting measurements with the individual results$\boldsymbol{n_i}$**.** It is assumed that the counts $\boldsymbol{n_i}$ were obtained under identical conditions and for the same counting time; thus, their differences are solely due to the statistical nature of radiation measurements. Each number $\boldsymbol{n_i}$ has a standard deviation$\sigma_i = \sqrt{n_i}$. The average of this series of measurements is:

$$\bar{n} = \frac{1}{N}\sum_{i=1}^{N} n_i \tag{2.42}$$

The standard error of $\bar{n}$ can be calculated:

The average $\bar{n}$ is the best estimate of a Poisson distribution of which the outcomes n_i are members. The standard deviation of the Poisson distribution is $\boldsymbol{\sigma = \sqrt{\bar{m}} = \sqrt{\bar{n}}}$. The standard error of the average is:

$$\sigma_{\bar{n}} = \frac{\sigma}{\sqrt{N}} = \sqrt{\frac{\bar{n}}{N}} \tag{2.43}$$

2.8.1 The Standard Error of Counting Rates

In practice, the number of counts is usually recorded in a scaler, but what isreported is the counting rate, i.e., counts recorded per unit time. The following symbols and definitions will be used for counting rates.

G = number of gross counts in time $\mathrm{t_G}$ with the sample present,

B = number of background counts in time $\mathrm{t_B}$, without the sample,

$g = \frac{G}{t_G}$ = gross counting rate , $b = \frac{B}{t_B}$ = background counting rate

r = net counting rate = $g - b$

The standard error of the net counting rate can be calculated by:

$$\sigma_r = \sqrt{\sigma_g^2 + \sigma_b^2} = \sqrt{\frac{G}{t_G^2} + \frac{B}{t_B^2}} \tag{2.43}$$

It is important to notice that in the equation for the net counting rate, the quantities *G*, *B*, t_G, and t_B are the independent variables, not g and b.

Chapter 3

MATERIALS AND METHOD

In this chapter, we briefly review the experimental methods and equipment that we use for measurements of radiation in high exposer building materials. Whereas, the high exposer building material is a family of the igneous rocks. For example quartz, feldspar and glassy groundmass, that we normally know as granite stones. Today, anywhere in the world people are using granite stones as internal cover and internal decoration.

The present research is a survey and measurement of terrestrial radionuclides such as Th-232, U-238, Ra-226, K-40 and Rn-222 gases in granite stones. After that, in the next subsection we will discuss about effective dose and its hazards. At the end, we will present the two methods of radon exhalation rate.

3.1 Determination of the Specific Activity Concentrations

3.1.1 Samples Preparation

The collected samples were crushed to fine powder with a particle size 1 mm and sieved in order to homogenise it and remove big size (Fig.3.1). The samples were then dried at $100\ C^0$ for 24 h to remove the wetness. The powdered samples were packed in a standard Marinelli beaker [24] and after properly tightening the cover; the samples were sealed and left for 30 d before counting by gamma spectrometry in order to ensure that the daughter products of ^{226}Ra and ^{232}Th are in secular equilibrium with their respective parent radionuclides [25].

When the radionuclides were in equilibrium, the activity concentration of each daughter was equal to the initial isotope of the series [26].

3.1.2 Measurement of Samples

The gamma spectrometry systems are used to measurements of samples in this research. This system include a high-resolution gamma spectrometer HPGe detector based on a coaxial P-type, 1.80 keV FWHM for the 1332 keV gamma-ray line of ^{60}Co and a relative photopeak efficiency of 80 % and energy resolution. This system coupled to a high count-rate Multi Task 16k MCA card. Commercial software Gamma 2000 from Silena-Italy was used for data analysis. The environmental background (B.G) achieved by blank sample was subtracted from each spectrum. A diagram of the experimental setup used is shown in Fig.3.2. The gamma B.G level at the counting room was determined with an empty Marinelli beaker washed with dilute HCl and distilled water. The background was measured under the same conditions of the measurement of the samples. The MDA for each measured radionuclide was established from the background radiation spectrum for a counting time of 80 000 s and the values were 0.7, 0.6 and 9.1 Bq kg^{-1} for ^{226}Ra, ^{232}Th and ^{40}K, respectively.

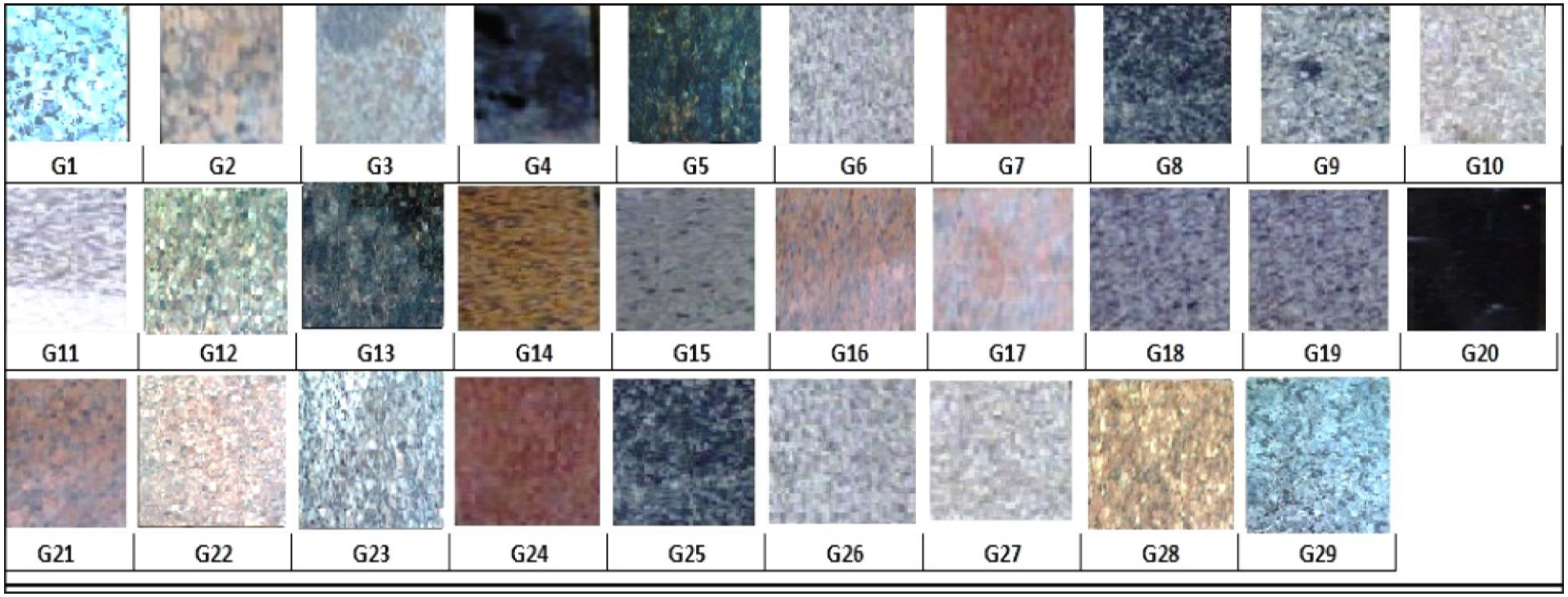

Figure 3.1. Granite samples used in the study

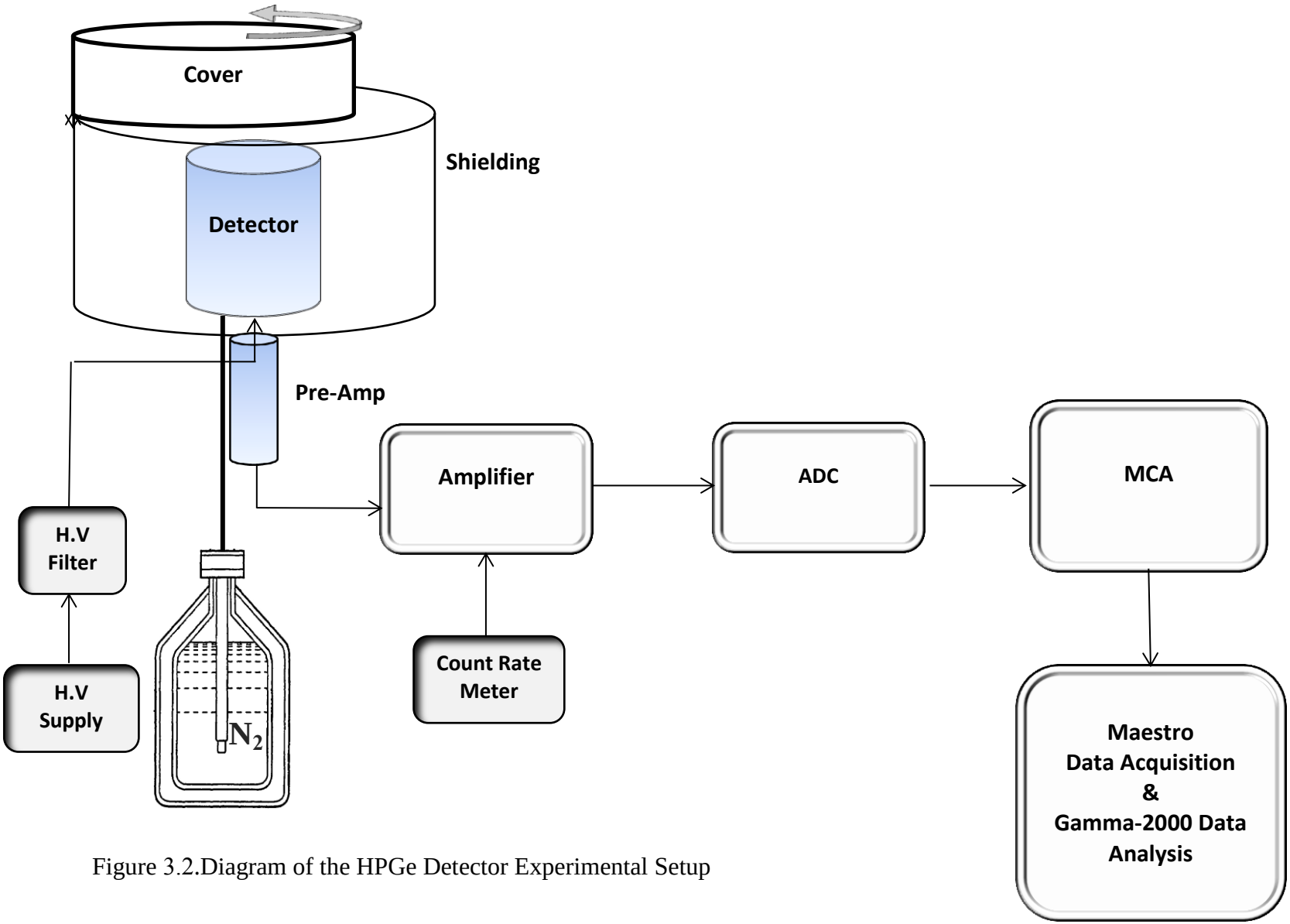

Figure 3.2.Diagram of the HPGe Detector Experimental Setup

The energy calibration was performed using 4 standard point sources, containing ^{241}Am, ^{133}Ba, ^{137}Cs and ^{60}Co, covering an energy range of approximately 60–1500 keV. This system was calibrated for efficiency over the photon energy range 180–2000 keV by using International Atomic Energy Agency (IAEA) reference materials. This material were such as RGTh-1 (Th-ore), RGU-1 (U-ore) and RGK-1 in the same Marinelli beakers. The counting time for gamma measurements system was 80 000 s. The ^{232}Th activities concentration were measured by taking the ^{228}Ac (338.40, 911.07 and 968.90 keV) photopeaks. Also another radionuclide is ^{212}Pb with photopeak energy (238.63 keV). Similarly, ^{226}Ra activities were measured from the activity of its short-lived daughters ^{214}Bi at 609.3 keV and ^{214}Pb at 295.2 and 351.9 keV. Activities concentration were determined with photopeak 1460.83 keV that directly emitter from ^{40}K radionuclide [27].

The activity concentration levels in mentioned radionuclides are computed by comparing method using above-mentioned reference materials. The activity concentration of each radionuclide is expressed in units of Becquerel per kilogram (Bq/kg) in dry weight come from the net counting rate of related gamma-line deducted from background (in counts per second), assuming the calibration efficiency of the HPGe detector for that line, which is the absolute transition probability of gamma ray.

3.2 Safety Indices Calculation

According UNSCEAR (1982) and EC (1999) [1, 28], three indices are able to calculate from special activity concentration. These three indices are such as radium

equivalent activity(Ra_{eq}), external hazard index (H_{ex}) and internal hazard index (H_{in}) that in the following described.

3.2.1 Radium Equivalent Activity (Ra_{eq})

The(Ra_{eq}), concept allows a single index or parameter to describe the gamma ray emission from different combination of U (i.e. Ra), Th and K in a material. The (Ra_{eq}) activity was considered (1, 29) as:

$$Ra_{eq} = a\,A_{Ra} + b\,A_{Th} + cA_K \tag{3.1}$$

where ^{226}Ra, ^{232}Th and ^{40}K specific activities are the A_{Ra}, A_{Th} and A_K, respectively. The effect constant parameters a, b, c are equal 1, 1.43, and 0.077 respectively [30].

According to the Ref. 27 the maximum value of Ra_{eq} in building materials must be, <370 Bq kg^{-1} for safe use, i.e. to keep the external dose under 1.5 (<1.5 mSvy^{-1}) [27].

3.2.2 External Hazard Index H_{ex}

The H_{ex} estimates the potential radiological hazard posed by different samples. This parameter is a dimensionless quantity and a safety criterion for materials radiation applying for is that $H_{ex} \leq 1$ [31]. The H_{ex} caused by the gamma radiation of the under-test granite samples are calculated by the following criterion equation:

$$H_{ex} = \frac{A_{Ra}}{370} + \frac{A_{Th}}{259} + \frac{A_K}{4810} \leq 1 \tag{3.2}$$

where the activity concentrations of ^{226}Ra, ^{232}Th and ^{40}K are appear by A_{Ra}, A_{Th} and A_K, respectively.

3.2.3 Internal Hazard Index H_{in}

The most internal exposure is from radon and its products that are concentrated in indoor places. The H_{in} estimates of potential radiological hazard are expressed by the internal hazard index H_{in} safety criterion [32, 33]. For the safe use of a material in the construction of dwellings, H_{in} should be less than unity [32] and satisfy the following criterion:

$$H_{in} = \frac{A_{Ra}}{185} + \frac{A_{Th}}{259} + \frac{A_K}{4810} \leq 1 \qquad (3.3)$$

where the activity concentrations of ^{226}Ra, ^{232}Th and ^{40}K (Bq/kg) , are A_{Ra}, A_{Th} and A_K parameter, respectively.

3.2.4 Gamma Activity Concentration Index $I_{\gamma r}$

The gamma activity concentration index ($I_{\gamma r}$) parameter (representative level index) is extracted from following equation [28, 34]:

$$I_{\gamma r} = \frac{A_{Ra}}{300} + \frac{A_{Th}}{200} + \frac{A_K}{3000} \qquad (3.4)$$

here the activity concentrations of ^{226}Ra,^{232}Th and ^{40}K (Bq /kg), are A_{Ra}, A_{Th} and A_K parameters, correspondingly.

The gamma activity concentration index $I_{\gamma r} \approx 2$ match an exception dose criterion limit (0.3 mSv y^{-1}), when the gamma index $I_{\gamma r} \approx 6$ met the dose criterion of 1 mSv y^{-1} [28].

3.3 Calculation of Radon Exhalation and Gamma Radiation Dose Rate

Gamma radiation due to granite building materials has been surveyed by applying a high purity gamma detector system. Health hazards from gamma radiation doses due to granite and radon concentration have been calculated by "RESRAD 6.5" computer code.

3.3.1 Exposure to Radon

The indoor radon exposure has surveyed in the room, so in this model supposes that radon release from other materials brought into the room is insignificant and radon gas due to building materials is mixed with the air uniformly. Therefore, the concentration of ^{222}Ra in the room is obtained by solving the following equation [35].

$$\frac{\partial C_i(t)}{\partial t} = E_X \frac{S}{V} + C_0\lambda_v - C_i(\lambda_{Rn} + \lambda_v) \tag{3.5}$$

In this equation $C_i(t)$ is the ^{222}Ra activity concentration in the room at time t in Bq m^{-3}, E_X is the radon exhalation rate (Bq m^{-3} h^{-1}), S is the exhaling surface area (m^2), V is the volume of room (m^3), λ_{Rn} is the decay constant of ^{222}Ra and λ_v is the air exchange rate at time t in h^{-1}. This value is between 0.1 h^{-1} to 3 h^{-1} for residences room. The air exchange rate value is selected 0.5 h^{-1} according UNSECAR report that is recommended for residential mechanical ventilation systems [1]. The value C_0 is the outside ^{222}Ra concentration with the world average value 10 Bq /m^3 in the outside air [36].

$$C_{i=} \frac{E_x S/V + C_0\lambda_v}{(\lambda_{Rn} + \lambda_v)} \tag{3.6}$$

The ^{222}Ra exhalation rate per square (m^2) can be calculated by concentration of ^{226}Ra value [37]:

$$E_x = \frac{1}{2} A_{Ra} \lambda \rho \eta d \tag{3.7}$$

where ρ the density (kg/m^3), η is the emanation coefficient, and d is the wall thickness (m). The emanation coefficient value was reported between 2.54 % to 6.04 % (average: 4.29%) for granite stones [38].

We suppose the building materials are in dry condition and radon transport is in this condition; therefore, Eq (3.7).

3.3.2 External Gamma-ray Radiation

The indoor radon dose rate is calculated for a rectangular source with uniform density and activity concentration in this research. Also, the external gamma-ray dose rate parameter was calculated in standard room (5.0 m ×4.0 m ×2.8 m) by summing the apart calculated gamma-ray dose rates by walls and floor. Therefore, we calculated external gamma-rays in two states. Firstly, the external gamma-ray dose rate was calculated for walls and floor covered with granite 3.0 cm thicknesses according to reports by Mustonen [39]. Secondly, the gamma-ray dose rate was due to the floor covered by granite stones in residential areas, work offices and schools for decorative purposes.

The specific indoor dose rate depends on wall thickness and density of material. It does not depend on the position in the room [40,41]. In this work, the density of granite was calculated for all samples and we obtained 2580 kg m^{-3}, on the average.

The granite in markets is usually 3.0 cm thick and (30.0 cm × 50.0 cm) in dimensions.

We also performed dose rate conversion factors calculations based on the "AESRAD 6.5" code for floor covered with 3.0 cm thick granite. The free-in-air absorbed dose value in the middle of the room can be expressed as [35]:

$$D(nGy.h^{-1}) = K_K A_K + K_{Ra} A_{Ra} + K_{Th} A_{Th} \quad (3.8)$$

where D is the absorbed dose in the center of the room, A_K, A_{Ra} and A_{Th} are the activity concentration (Bq kg^{-1}) of ^{40}K, ^{226}Ra and ^{232}Th, respectively. Coefficients of K_K, K_{Ra} and K_{Th} are their dose conversion factors in nGy h^{-1} per Bq kg^{-1}.

3.3.3 Effective Dose Rate

The annual effective doses calculation, from absorbed dose in air to effective dose one has to take into account the conversion coefficient and the indoor occupancy factor. According the UNSCEAR's recent reports [7,37], a value of the conversion coefficient from absorbed dose in air to effective dose received by adults is 0.7 Sv y^{-1},and the indoor occupancy factor is 0.8. These parameters are assumes that 20 percent of the time is spent outdoors averagely. The effective dose E (in mSvy^{-1}) is calculated by the following formula [42]:

$$E(mSv\ y^{-1}) = D.T.F \quad (3.9)$$

where D is the absorbed dose (nGy h^{-1}), F is the conversion factor (0.7×10^{-6} Sv Gy^{-1}) and T is the indoor occupancy time (0.8 ×24 h ×365.25 d ≅7010 h y^{-1}).

3.4 Comparison of Passive and Active Methods for Radon Exhalation Rate

The radon exhalation rates and radon concentrations in granite stones were measured by means of gamma-spectrometry system with a high purity Germanium HPGe detector (passive method) and an AlphaGUARD model PQ 2000 (active method). For standard rooms (4.0 m×5.0 m× 2.8 m) where ground and walls have been covered by granite stones, the radon concentration and the by two methods were calculated.

3.4.1 Passive Method

All the collected samples after crashed, sieved with 200-μm mesh; dry weighed and closed in Marinelly beakers geometries (m=1000 gr) [24]. After these process samples are stored for 28 days before counting in order that obtain equilibrium between radum-226 and radon-222 and its decay products. Finally, samples were measured by means a coaxial P-type high purity Germanium (HPGe) detector, with a relative photopeak efficiency of 80 % to NaI detector. The energy resolution of this system was 1.80-keV FWHM for the 1332-keV gamma-ray line of ^{60}Co. The energy calibration we used four standard point sources, containing ^{241}Am, ^{133}Ba, ^{137}Cs and ^{60}Co, covering an energy range of ~60– 1500 keV. The system was adjusted for efficiency between photon energy range of 186–2700 keV using the International Atomic Energy Agency reference materials (RM) such as RGTh- 1(Th- ore), RGU-1 (U-ore), and RGK-1 packed in the same Marinelli beakers. The counting time for this system was 80,000 s. Before the sample counting, the environmental background radiation was determined with counting an empty Marinelly geometry under same conditions for samples (background) at the laboratory site.

The ^{226}Ra activity concentration was calculated with their total uncertainties for each the measured samples. Activities of ^{226}Ra were calculated from the activity of its daughters such as ^{214}Pb at 295.2 and 351.9 keV, and ^{214}Bi at 609.3 keV [43]. To compare the results of uncertainty, standard materials such as Soil-375 (20 Bq kg^{-1} ^{226}Ra concentration) and RGU-1 (U ore) (4940 Bq kg^{-1} ^{238}U concentration) were used [44].

From the measured values of the ^{226}Ra concentration, the R.E.R per unit area can be calculated by [37]:

$$E_x = \frac{1}{2} A_{Ra} \lambda \rho \eta d \tag{3.10}$$

Here A_{Ra} is ^{226}Ra (Bq kg^{-1}) concentration, λ is Rn decay constant (7.567×10^{-3} h^{-1}), ρ is the density (kg/m^3), d is the wall thickness (m), and η is the emanation constant. The emanation coefficient value was to be reported between 2.54 % to 6.04 % (average: 4.29%) for granite stones [38]. This parameter is one important instance in uncertainty. The emanation constant is dependent on the porosity, size and form of the material.

The building materials are wet the transport condition is different; therefore, Eq (3.10) are used only for dry conditions [37].

3.4.2 Active Method

To measure Rn gas, an AlphaGUARD model PQ 2000 pro (SAPHYM Co) was used. This device works based on the passing of Rn gas from a filter to the ionization

chamber. Radon surveys were carried out in a special cubic chamber (70×50×60 cm) with different changeable walls. One set of floor and half of each wall was covered with the most common granite stones used in Iran. Each sample was put into a special cubic chamber to reach equilibrium between ^{222}Rn and its daughters. After the balance state between radon and its daughters, the activity of ^{222}Rn exhaled from each building material sample measured for an accumulated time of 60 min. The schematic diagram in Fig.3.3 shows radon exhalation rate measured by active setup method.

The background value was later deducted from the radon concentration of each sample. All the samples were measured after one hour in (N= 5-6) times to get average results. By Alpha View/Expert software, final activity of Rn gas (A_0) with decay correction was computed. Radon gas exhalation rate was computed as [45]:

$$E_x = A_0 \lambda \left(\frac{V}{F}\right) \tag{3.11}$$

where E_x, ^{222}Rn gas exhalation rate in unit Bq m^{-2} h^{-1}; A_0, final activity of ^{222}Rn gas in unit Bq m^{-3}; λ , ^{222}Rn decay constant (7.567. 10^{-3} h^{-1}); V, emanation container volume (m^3); and F, area of each sample (m^2).

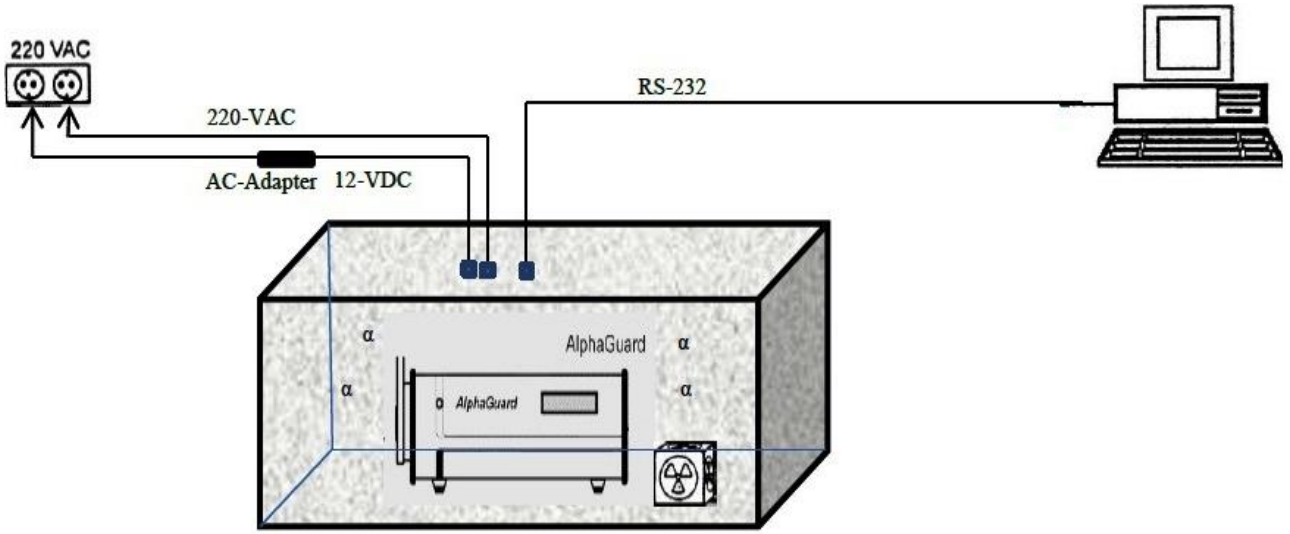

Figure 3.3. Schematic Diagram Showing the Radon Exhalation Measurements of Granite Samples by Active Setup Method

Chapter 4

RESULTS AND DISCUSSION

In this chapter, we present experimental results and discussion that we obtained during this research. Also, we compared two methods of radon concentration in standard dwelling.

4.1 Activity Concentration (A)

The activity concentration of ^{232}Th, ^{226}Ra and ^{40}K in different commercial granite used as building materials in Iran are shown in Table 4.1. In these samples the range of radium equivalent activity were found between 20.34-100.70 Bq kg^{-1}. The (Ra_{eq}), (H_{in}) and (H_{ex}) to quantify the internal exposure to radon and its daughter products, as well as the gamma activity concentration index $I_{\gamma r}$ for each sample are presented in Table 4.2.

Furthermore, the average of these values was calculated and given in Table 4.2. The obtained average values for studied granite samples are 272.32 Bq/kg , 0.74, 0.93 and 1.02 for Ra_{eq} , H_{ex}, H_{in} and $I_{\gamma r}$, respectively. According to the NCRP (20), worldwide estimated levels of ^{232}Th, ^{238}U and ^{40}K concentrations in granite as building material are 8, 63 and 1184 Bq kg^{-1}, respectively. In this study, the activity of ^{232}Th, ^{226}Ra and ^{40}K in the surveying samples were between 18 to 178, 6 to 160 and 556 to 1539 Bq kg^{-1} respectively. The average values of these radionuclides were 76, 72 and 1193 Bq kg^{-1}, respectively.

Maximum A of ^{232}Th, ^{226}Ra and ^{40}K were 178±11 Bq kg^{-1}, 160±8 Bq kg^{-1} for (G-17) (China) and 1539±51 Bq kg^{-1} for (G-6) (Iran), respectively.

4.2 Radium Equivalent, External Internal Hazard Indices

The calculation result of the (Ra_{eq}) for the studied granite samples are shown in Table 4.2. The result range are between 100.70 Bq kg^{-1}(G-2) (Iran) to 520.34 Bq kg^{-1}(G-17) (China). The maximum value of radium equivalent activities was 520.34 Bq kg^{-1}. In this research we found that the calculated Ra_{eq} is under the maximum recommended value (370 Bq kg^{-1}), except in two samples. It is assumed that 259 Bq kg^{-1} of ^{232}Th, 370 Bq kg^{-1} of ^{226}Ra and 4810 Bq kg^{-1} of ^{40}K product the same gamma-ray radiation dose rate (26, 46).

External hazard index H_{ex} ranged between 0.27 and 1.41. According to the safety criterion, average external hazard index must be less than unit. It means that the obtained values of H_{ex} for the various granite samples, exhibition that the safety criterion were met by 15 samples. The internal hazard index values for five granite samples are higher than unity. According the European Commission (EU) reports, building material index H_{in}should be smaller than unit. The average calculated values of (H_{in}) for the investigated samples ranging from 0.34 to 1.84 are presented in Table 4.2. On the basis of the obtained activities of ^{232}Th, ^{40}K and ^{226}Ra in studied granite samples, gamma activity concentration index $I_{\gamma r}$, according to the European Commission (EU) [28] as a screening tool for identifying building materials has been obtained by using equation (3.4).

Table 4.1.The Specific Activity Concentrations in Studied Granite Samples

Sample No.	Commercial name	Origin	Activity (Bq/kg)		
			^{232}Th	^{226}Ra	^{40}K
G-1	Brown india	India	85±2	11±2	1220±19
G-2	Chayan sable	Iran	23±1	25±3	556±27
G-3	Tekab	Iran	95±3	69±4	690±24
G-4	Nehbndan birjand	Iran	172±8	152±12	1385±39
G-5	Peranshahr	Iran	62±6	69±2	1422±17
G-6	Torbat hydaryeh	Iran	33±3	40±2	1539±51
G-7	Natanz	Iran	84±4	71±2	688±23
G-8	Morvared mashhad	Iran	52±2	42±1	848±11
G-9	Akbatan hamedan	Iran	98±5	95±5	1374±36
G-10	Sangeh alamot	Iran	59±4	91±2	1319±20
G-11	Garmez yazd	Iran	22±1	55±2	1124±34
G-12	Balloch zahedan	Iran	45±3	71±4	1077±46
G-13	Morvared sabz	Iran	81±4	52±3	1211±54
G-14	Khoramdareh	Iran	75±4	131±3	1451±31
G-15	Garmez golrez	China	105±9	88±4	1505±28
G-16	Gal excei	India	18±2	6±1	1490±10
G-17	Garmez goldorosht	China	178±11	160±8	1374±41
Min-Max			18 - 178	6 - 160	556 - 1539
Average			76±9	72±2	1193±23

Table 4.2.The Ra_{eq}, H_{ex} H_{in} and $I_{\gamma r}$ Indices for Studied Granite Samples

Sample No.	Commercial name	$Ra_{eq}(Bq\ kg^{-1})$	H_{ex}	H_{in}	$I_{\gamma r}$
G-1	Brown india	226.49	0.61	0.64	0.87
G-2	Chayan sable	100.70	0.27	0.34	0.38
G-3	Tekab	257.98	0.70	0.88	0.94
G-4	Nehbndan birjand	504.61	1.36	1.77	1.83
G-5	Peranshahr	267.15	0.72	0.91	1.01
G-6	Torbat hydaryeh	205.69	0.56	0.66	0.81
G-7	Natanz	244.10	0.66	0.85	0.89
G-8	Morvared mashhad	181.66	0.49	0.60	0.68
G-9	Akbatan hamedan	340.94	0.92	1.18	1.26
G-10	Sangeh alamot	276.93	0.75	0.99	1.04
G-11	Garmez yazd	173.01	0.47	0.62	0.67
G-12	Balloch zahedan	218.28	0.59	0.78	0.82
G-13	Morvared sabz	261.08	0.71	0.85	0.98
G-14	Khoramdareh	349.98	0.95	1.30	1.30
G-15	Garmez golrez	354.04	0.96	1.19	1.32
G-16	Gal excei	146.47	0.40	0.41	0.61
G-17	Garmez goldorosht	520.34	1.41	1.84	1.88
Average		272.32	0.74	0.93	1.02

4.3 Dose-Rate Conversion Factors

The DRCF were also calculated for a standard room. We have shown the result in Table 4.3 compared with standard rooms [42]. Table 4.3 presents the results calculated for two standard model rooms: the first model is that used in most reports [35] and the other model is that surveyed in this research.

The results of the radon exhalation rate (E_x), radon concentration (C_i) and absorbed dose (D) were calculated from the obtained results.

4.4 Radon Exhalation Rate, Radon Concentration and Absorbed Dose Results

The results presented in Table 4.4 are for all samples that are usually used in Iran. The radon exhalation rate Ex values, were found to be in the range 0.32+0.01 to 7.86+ 1.65 Bq m^{-2} h^{-1} with an average of 3.71+0.80 Bq m^{-2} h^{-1}, as shown in Fig 4.1. The radon concentrations are due to exhalation from material shown in Fig.4.2. This results are accordance with others author findings reports [47, 48].

The minimum and maximum values of absorbed dose rates (dD/dt) are 3.84–68.02 and 2.29–39.99 nGy h^{-1} in Model 1 and Model 2 rooms, respectively. Table 4.4 shows that the EGDR in granites depends on the type of granite stones used in the inner walls and floors of buildings. For the calculation of radon gas exhalation rate, it was assumed that the room is equipped with mechanical ventilation systems ($\lambda_v = 0.5\ h^{-1}$).Values of $\lambda_v < 0.1$ represent cases of extremely poor ventilation.

According to the latest scientific data of World Health Organization (WHO) report, on health effects of indoor ^{222}Rn have given an indoor ^{222}Rn concentration reference level of 100 Bq m^{-3}[11]. The above values for radon gases the reference level residences reported in the ICRP recommendations was 300–600 Bqm^{-3}. According to estimations here, if a room is adapted with mechanical ventilation systems ($\lambda_v = 0.5\ h^{-1}$) as given here, all granite samples would produce radon concentration, 100 Bqm^{-3}. If one adapts a poorly ventilated Model 1 room ($\lambda_v = 0.1h^{-1}$), only two samples G-14 and G-17 yield values greater than the reference level (100 Bqm^{-3}) with regard to health effects [11].

Table 4.3 The Conversion Factors for the Calculation of Absorbed Dose (D)

Configuration of rooms	**Structures**	**Thickness (cm)**	**dose rate (nGy h^{-1} / Bq kg^{-1})**		
			^{226}Ra	**^{232}Th**	**^{40}K**
Model 1[a]	Floor and walls	3.0	0.17	0.20	0.013
Model 2 [b]	Only floor covered with granites	3.0	0.09	0.12	0.008

[a] Walls and floor covered with granites (Markkanen 1995)

[b] Floor covered with granites (calculated with "RESRAD 6.5" computer code http://www.ead.anl.gov/resrad in this research)

Table 4.4. The Radon Exhalation Rate (E_x), Radon Concentration (C_i) and Absorbed Dose Rate (dD/dt) from Different Types Of Granites Used in Iran (in Dry -Condition)

No	Sample code	Region	Commercial name	E_x[a] ($Bqm^{-2}h^{-1}$)	C_i[a] ($Bq\ m^{-3}$) (λ_v=0.5 h^{-1})		dD/dt ($nGy\ h^{-1}$)	
					Room Model 1	Room Model 2	Room Model 1	Room Model 2
1	G 2	Iran	Chayan sable	1.31±0.26	13.10	10.77	14.59	8.68
2	G 3	Iran	Tekab	4.32±0.81	20.56	12.89	36.81	21.60
3	G 4	Iran	Nehbndan birjand	7.64±1.02	28.79	15.23	68.02	39.99
4	G 5	Iran	Peranshahr	3.30±0.65	18.03	12.18	39.28	23.40
5	G 6	Iran	Torbat hydaryeh	2.26±0.32	15.45	11.44	19.44	11.46
6	G 7	Iran	Natanz	5.99±1.20	24.69	14.07	40.19	23.42
7	G 8	Iran	Morvared mashhad	1.58±0.32	13.76	10.96	29.62	17.82
8	G 9	Iran	Akbatan hamedan	2.03±0.48	14.87	11.28	40.94	24.54
9	G 10	Iran	Sangeh alamot	3.81±0.77	19.30	12.54	37.74	22.37
10	G 11	Iran	Garmez yazd	3.43±0.65	18.35	12.27	32.90	19.46
11	G 12	Iran	Balloch zahedan	2.71±0.44	16.57	11.76	34.65	20.62
12	G 13	Iran	Morvared sabz	2.37±0.69	15.72	11.52	38.01	22.76
13	G 14	Iran	khoramdareh	7.86±1.65	29.32	15.38	61.91	36.32
14	G 19	Iran	Chayan sable	1.84±0.41	14.42	11.15	25.63	15.32
15	G 20	Iran	Tekab	4.24±0.88	20.35	12.83	39.55	23.30
16	G 22	Iran	Trasheh sfed	7.30±1.71	27.94	14.99	58.37	34.23
17	G 24	Iran	Morvared sabz	1.54±0.59	13.65	10.93	14.22	8.36
18	G 27	Iran	Hekmtaneh	3.41±0.80	18.31	12.25	38.17	22.61
19	G 28	Iran	Sangeh lorestan	2.72±0.58	16.59	11.77	17.01	9.87
20	G 29	Iran	Alborz	5.66±0.66	23.87	13.83	54.72	32.27
21	G 1	India	Brown india	0.78±0.03	11.77	10.40	34.65	20.92
22	G 16	India	Gal excei	0.32±0.01	10.64	10.07	3.84	2.29
23	G 15	China	Garmez golrez	5.96±0.94	24.61	14.04	45.61	26.76
24	G 17	China	Garmez goldorosht	7.79±1.23	29.16	15.34	65.93	38.71
25	G 18	China	Golzard	4.62±0.89	21.30	13.10	37.27	21.95
26	G 21	Armenia	Khalkhali	5.02±1.01	22.30	13.39	40.26	23.66
27	G 23	Pakistan	Goldar seyah	2.85±0.47	16.92	11.86	32.98	19.53
28	G 25	Turkish	Greh dash	1.19±0.13	12.81	10.69	12.95	7.67
29	G 26	Turkmenistan	Yazi dash	3.81±0.81	19.30	12.54	36.67	21.69
Average				3.71±0.80	19.05	12.46	36.27	21.43
Min - Max				0.32±0.01 – 7.86±1.65	10.64-29.32	10.07-15.38	3.84-68.02	2.29-39.99

[a] Uncertainties are given within 1 standard deviation

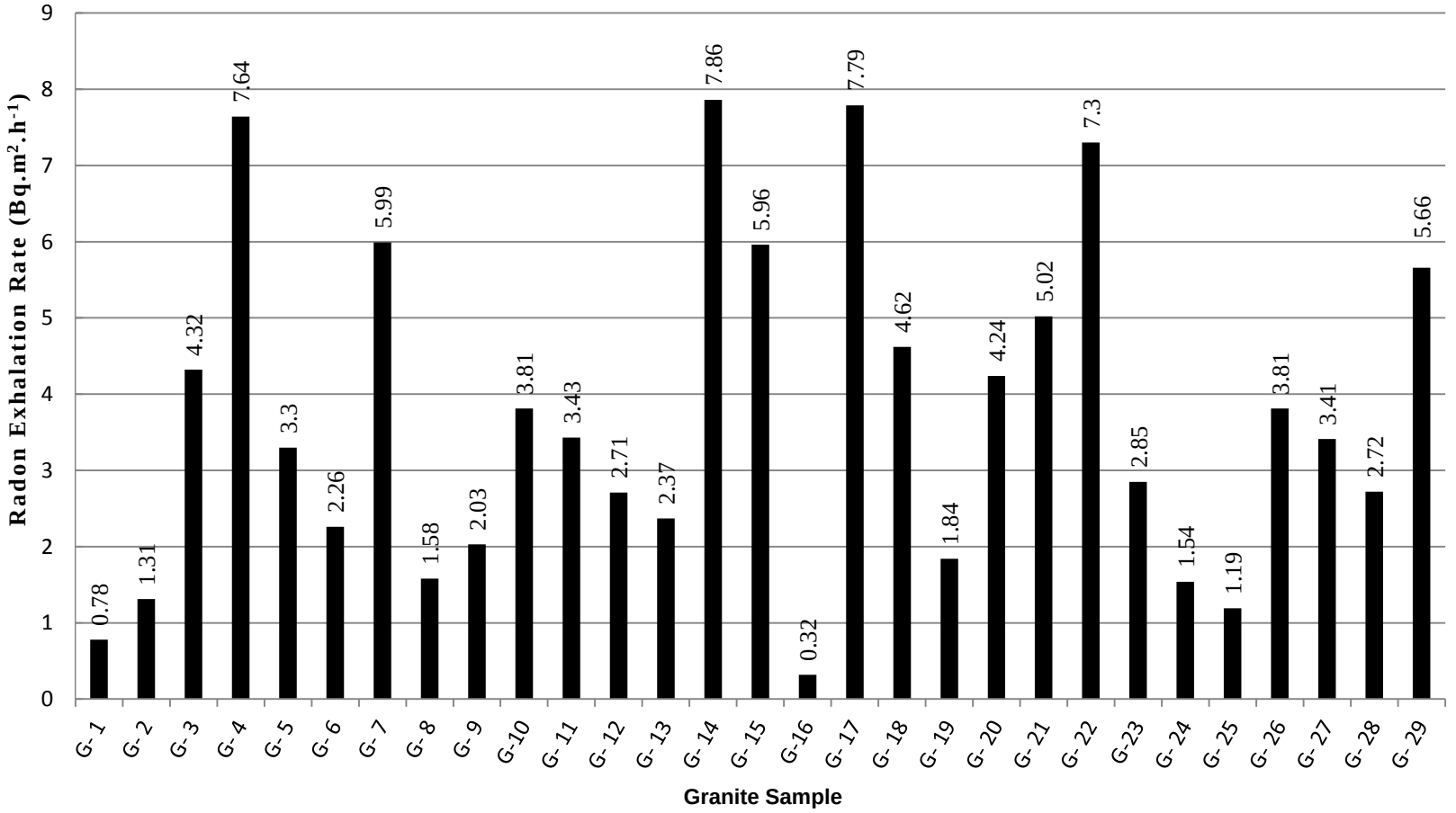

Figure 4.1. The radon exhalation rate in studied granite samples

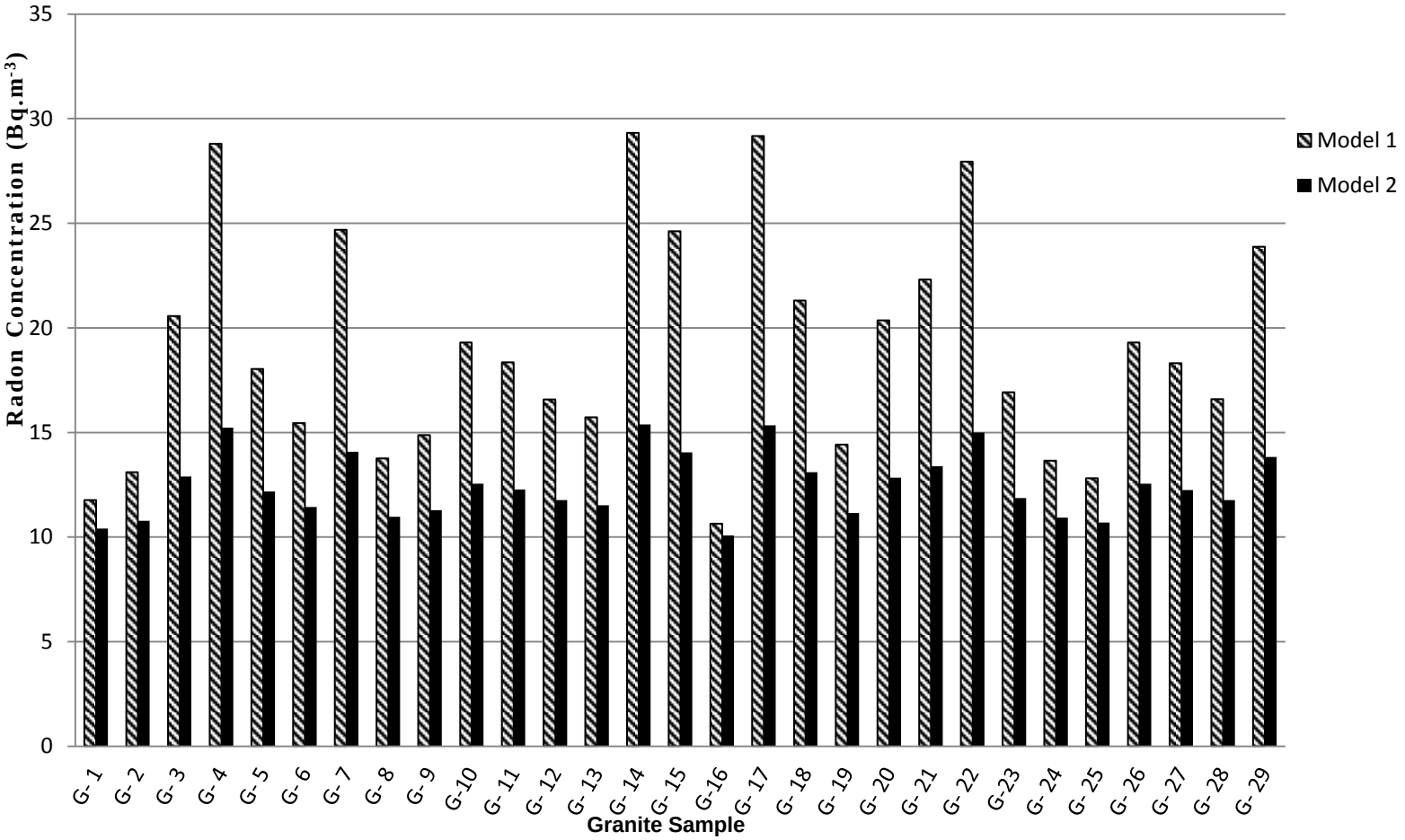

Figure 4.2. The radon concentration in two model dwelling with mechanical ventilation systems (λ_v=0.5 h^{-1})

4.5 The Radon Exhalation Rate by the Passive and Active Methods

The ^{222}Rn exhalation rate by the passive and the active methods in different commercial granite stones are shown in Table 4.5. The range of the radon exhalation rate was found to be 1.31–7.86 and 2.13–8.74 $Bqm^{-2}h^{-1}$ in the passive and active methods, respectively. The mean radon exhalation rate in the passive and active methods is 3.76 and 4.59 Bq m^{-2} h^{-1}, respectively.

Figure 4.3 shows when compared the results of passive and active methods. In total, data collected from active method is higher than for data collected from passive method. The results are similar with variation value of 22 % for all samples on average. Fig 4.4 shows the correlation between passive and active method results (correlation coefficient= 0.8696). In active method all of the measured data is higher than passive data measured except G4, G5 and G19 samples. Also, the comparison of uncertainty in the two techniques here shows that the precision in the passive method is less than that in the active method. This could be due to the determination of the emanation coefficient value. In the active setup, the result was obtained for bottom and half of each wall room covered with granite tiles. For standard room (4 m×2.8 m×5 m) without the ventilation system, the radon concentration range was obtained 218–1306 Bq m^{-3} with a mean of 625 Bq m^{-3}. The International Commission on Radiological Protection proposed action level of 500–1500 Bq m^{-3} for the Rn gas at workplaces (49). The Atomic Energy Organization (AEO) of Iran proposed an action level of 1000 Bq m^{-3} for dwellings(50). Therefore, only 15 % of granite tiles under studied are more than from action level proposed by

the AEO of Iran. The average radon exhalation rate observed here was similar to many other findings in investigations reported in the literature (14,16,19,52,53).

Table 4.5. The Radon Exhalation Rate (E_x), Using Passive and Active Method from Different Types of Granites

No	Sample code	Commercial name	E_x [a] ($Bqm^{-2}h^{-1}$)			
			Passive method	Uncertainty (%)	Active method	Uncertainty (%)
1	G 2	Chayan sable	1.31	20	2.13	13
2	G 3	Tekab	4.32	19	5.14	3
3	G 4	Nehbndan birjand	7.64	13	7.85	3
4	G 5	Peranshahr	3.30	20	3.12	13
5	G 6	Torbat hydaryeh	2.26	14	2.24	17
6	G 7	Natanz	5.99	20	6.45	7
7	G 8	Morvared mashhad	1.58	20	2.46	11
8	G 9	Akbatan hamedan	2.03	24	3.74	7
9	G 10	Sangeh alamot	3.81	20	4.05	12
10	G 11	Garmez yazd	3.43	19	5.21	8
11	G 12	Balloch zahedan	2.71	16	3.25	11
12	G 13	Morvared sabz	2.37	29	4.81	6
13	G 14	Khoramdareh	7.86	21	8.74	28
14	G 19	Chayan sable	1.84	22	3.79	12
15	G 20	Tekab	4.24	21	5.25	10
16	G 22	Trasheh sfed	7.30	23	8.42	7
17	G 24	Morvared sabz	1.54	21	2.96	13
18	G 27	Hekmtaneh	3.41	23	3.58	26
19	G 28	Sangeh lorestan	2.72	21	2.13	20
20	G 29	Alborz	5.66	12	6.57	6
	Average		3.76	20	4.59	11
	Max - Min		1.31 – 7.86	12-38	2.13 – 9.74	3-28

[a] Uncertainties are given within 1 standard deviation.

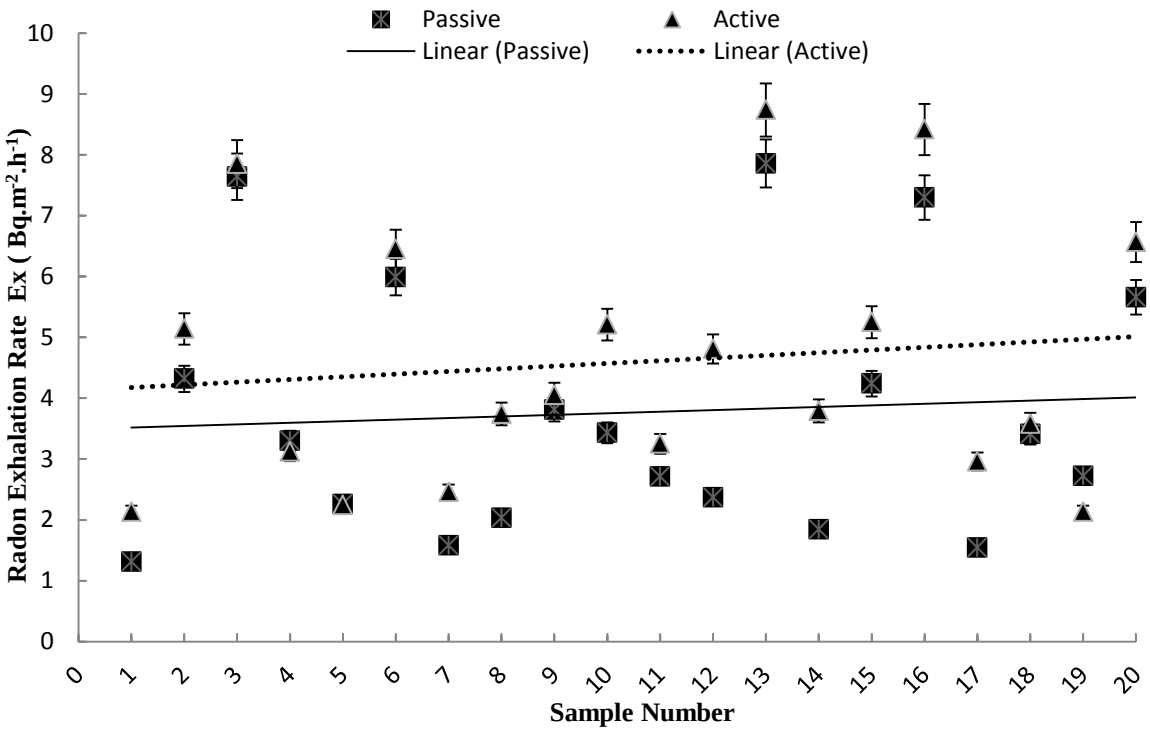

Figure 4.3. The radon exhalation rate measured by passive and active method

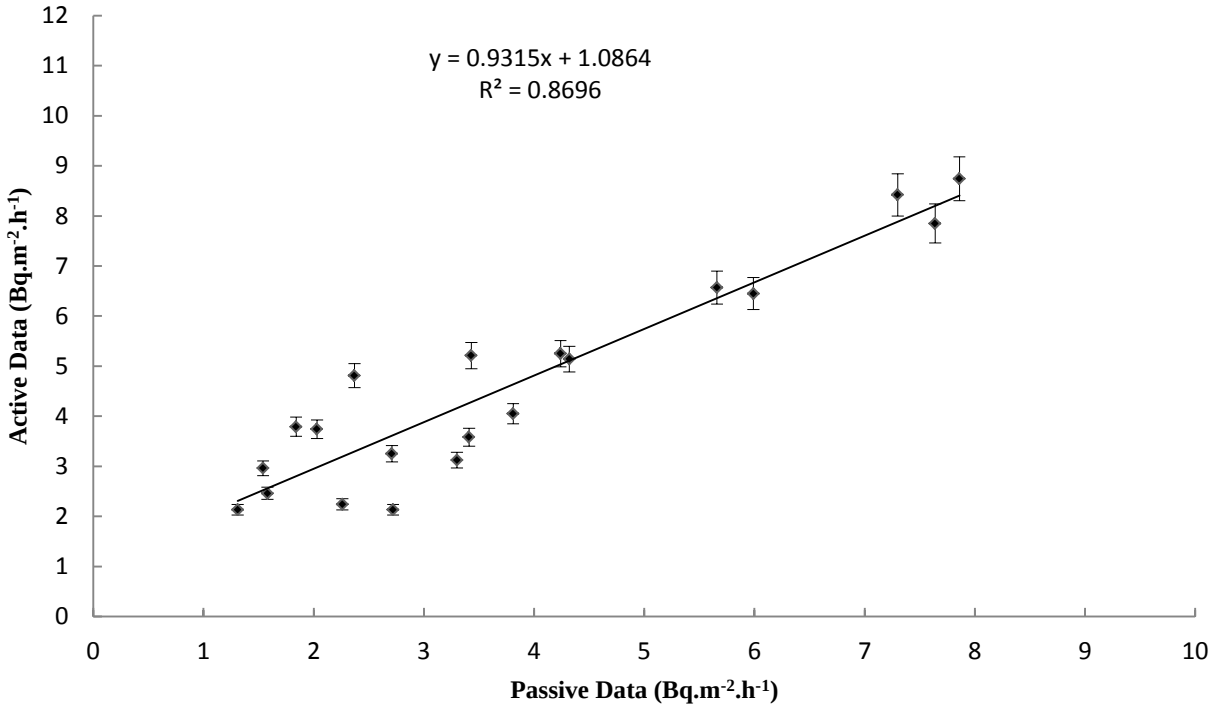

Figure 4.4 The correlation parameter between active and passive method.

Chapter 5

CONCLUSION

Environmental radioactivity and dose calculation should be fulfilled for granites where people must be exposed to radioactivity [54]. In considering the worldwide involve about the radioactivity contents of various construction materials such as granite stones, experimental measurements of the activity concentrations of various commercial granite types usually used in the Tehran region of Iran have been carried out. The average estimated Ra_{eq} is able to be compared with reported values for many countries in the world.

All of the samples under investigation were found to have hazard indices below 1.41 and 1.84 for the average H_{ex} and H_{in} hazard index, respectively. The H_{ex} index was calculated and found to be smaller than unit, averagely. Only two samples (G-N-I and G-RB-CH) were found to have average external hazard indices more than unity. It means the obtained values of Hex showing the safety criterion were met by 15 samples of 17. Five samples were found to have average internal hazard indices more than unity. So under the dose criterion and the calculation gamma activity concentration index values, the studied granite samples are satisfactory as superficial building materials with restricted use as countertops and decoration. It means that none of the samples exceeds from 300 $\mu Sv\ y^{-1}$ value of the dose limit. Hence, the use of these granite samples under

investigation in the building of residence is reasonable to be safe for resident, except the G4 and G17.

In recent years, there was an increased in modern building material using as decorative inner building materials. The granite stones include mainly of the ^{232}Th, ^{238}U series and also ^{40}K. The present work was intended to calculate the radon concentration (C_i), radon exhalation rate (E_x), and absorbed dose rate (dD/dt) levels in widely used existing granite samples locally. In total, two standard model rooms were assumed; Model 1 was surveyed by some references, while Model 2 is that employed in this research. The result shows that the radon exhalation rate (E_x) value ranges are 0.32± 0.01 to 7.86±1.65 Bq m^{-2} h^{-1} with an average of 3.71 ± 0.80 Bq m^{-2} h^{-1} (Fig. 4.1). These results were compared with values of the radon exhalation rates (E_x) in Greek [55], Brazilian [35] and Saudi Arabian [14] granite reports: 1.24±0.19 to 3.54±1.11, 0.60±0.10 to 21±2.3 and between 0.41±0.13 - 10.6±1.4 Bq m^{-2} h^{-1}, respectively.

The C_i value ranges are 10.64–29.32 and 10.07–15.38 Bq m^{-3} for both Model 1 and 2, respectively (Fig.4.2). Radon concentrations of granites in this study are compared with previously reported [56] results in houses in Iran. In this report, radon concentration measured ranges is 25 Bq m^{-3} averagely, in during the autumn season. Also, the absorbed dose rate (dD/dt) levels were 3.84–68.02 nGy h^{-1} for Model 1 and 2.29–39.99 nGy h^{-1} for Model 2, respectively. These results confirm that the air exchange rates and radon exhalation are significant parameters with regard to exposure from building materials. For poor ventilation ($\lambda_v =$

$0.1h^{-1}$) only 7 % granites under examination will present a C_i 100 Bq m^{-3}, 38% will present $50 < C_i < 100$ Bq m^{-3} and 55 % will present values <50 Bq m^{-3}.

The radon exhalation rates were evaluated in selected granite stones by using passive and active measuring techniques. The minimum and maximum values of the E_x in the passive method were as in GC1 and GT16 samples, respectively. Also, the minimum and maximum values of the E_x in the active method were as in GC1 and GK13 samples, respectively.

From the comparison of the two methods, the active method is a fast, simple and cheap but its low LLD range is a disadvantage, whereas, the passive method has a high LLD, which is an advantage. The disadvantage is that it takes a long time to get the results and partly dependent on the subsidiary parameter (emanation coefficient). The exhalation rates measured by the passive (gamma spectrometry) and active (AlphaGUARD setup) methods were compared. In total, the results are similar, with the active method being 22 % higher than the passive method. The correlation coefficient is R^2=0.8696 between the two methods.

REFRENCES

[1] UNSCEAR. (1982). United Nations Scientific Committee on the Effects of Atomic Radiation. Ionizing Radiation: *Sources and Biological Effects*. UN, 425-431.

[2] Hewamanna, R., Sumithrarachchi, C. S., Mahawatte, P., Nanayakkara, H. L. C. and Ratnayake, H. C. (2001). Natural Radioactivity and Gamma Dose from Sri Lankan Clay Bricks Used in Building Construction. *Appl. Radiat. Isot*. 54, 365–369.

[3] Khatibeh, A. J. A. H., Ahmad, N., Matiullah and Kenawy, M. A. (1997). Natural Radioactivity in Marble Stones- Jordan. *Radiat. Meas*. 28, 345–348.

[4] Evan, R. D. (1969). Engineer's Guide to Elementary Behavior of Radon Daughters. *Health Phys*. 17, 229–252.

[5] Burns, P. and Finch, R. (1999). Uranium, Mineralogy, Geochemistry and the Environment. In: Reviews in Mineralogy. *Mineralogical Society of America*, Vol. 38.

[6] NCRP 94. (1987). Estimates of Concentrations of Uranium, Thorium and Potassium in Building Materials, 284-291.

[7] UNSCEAR (2000). (United Nations Scientific Committee on the Effects of Atomic Radiation). *Sources and effects of Ionizing Radiation*. United Nation .

[8] NCRP, (2009). (National Council on Radiation Protection and Measurements). Ionizing radiation exposure of the population of the United States. *NCRP Report No. 160*, 283-290.

[9] UNSCEAR (1988b). (United Nations Scientific Committee on the Effects of Atomic Radiation). Exposure from Natural Sources of Radiation. *Report to ANNEX.A.*

[10] ICRP . (1999). (International Commission on Radiological Protection). Protection of the Public in Situations of Prolonged Radiation Exposure. *Elsevier Science* B.V. *ICRP Publication 82.*

[11] WHO. (2009).WHO Handbook on Indoor Radon: A Public Health Perspective. *World Health Organization*. WHO Press. p. 27

[12] Sundar, S. B., Ajoy, K. C., Dhanasekaran, A., Gajendiran, V. and Santhanam, R. (2003). Measurement of Radon Exhalation Rate from Indian Granite Tiles. in Proceedings International Radon Symposium, *Amer Assoc of Radon Sci and Technol*, Vol. II.

[13] Durrani, S.A. and Ilic, R. (1997). Radon Measurements by Etched Track Detectors: Applications to Radiation Protection. *Earth Sciences and the Environment World Scientific*.154-162.

[14] Al-Jarallah, M. I., Ur-Rehman, F., Musazay, M. S. and Aksoy, A. (2005).Correlation Between Radon Exhalation and Radium Content in

Granite Samples Used as Construction Material in Saudi Arabia. *Radiat. Meas*. 40, 625–629.

[15] Baradaran-Ghahfarokhi, M., Faghihi, R., Karami, M., Siavashpour, Z. and Owji, H. (2011). The Effects of Internal Wall Covering Materials on Hazards of Indoor Radon Concentrations in Houses of Iran. *Iran Red Crescent Med. J*. 13(9), 637–640.

[16] Keller, G., Hoffmann, B. and Feigenspan, T. (2011). Radon Permeability and Radon Exhalation of Building Materials. *Sci. Total Environ*. 272, 85–89.

[17] Petropoulos, N. P., Anagnostakis, M. J. and Simopoulos, S. E. (2002). Photon Attenuation, Natural Radioactivity Content and Radon Exhalation Rate of Building Materials. *J. Environ. Radioact*. 61, 257–269.

[18] Righi, S. and Bruzzi, L. (2006). Natural Radioactivity and Radon Exhalation in Building Materials Used in Italian Dwellings. *J. Environ. Radioact*. 88, 158–170.

[19] Allen, J. G., Minegishi, T., Myatt, T. A., Stewart, J. H., McCarthy, J. F. and Macintosh, D. L. (2010). Assessing Exposure to Granite Countertops—Part 2: *radon. J. Exposure Sci. Environ. Epidemiol.* 20(3), 263–272.

[20] NCRP 94. (1998). Estimates of Concentrations of Uranium, Thorium and Potassium in Building Materials. 412-415.

[21] D. Halliday.1955. Introductory Nuclear Physics, 2 nd Edition, John Wiley. *University of Pittsburgh*. 215-219.

[22] B. Alex Brown,. 2005, Nuclear Structure Physics. National Superconducting Cyclotron Laboratory and Department of Physics and Astronomy Michigan State University. 291-318.

[23] N.Tsoulfanidis, 1995. Measurement and Detection of Radiation. 2 nd, *University of Missouri-Rolla.*

[24] IEEE. (1997). IEEE Standard Test Procedures for Germanium Gamma-Ray Detectors. Approved by ANSI. *IEEE Std*:3251996 .

[25] Harb, S., El-Kamel, A. H., Abd El-Mageed, A. I., Abbady, A. and WafaaRashed. (2008). Concentration of U-238, U-235, Ra-226, Th-232 and K-40 for Some Granite Samples in Eastern Desert of Egypt. In: *Proceedings of the Third Environmental Physics Conference*, Aswan, Egypt, 19–23 February.

[26] Walley El-Dine, N., El-Shershaby, A., Ahmed, F. and Abdel-Haleem, A. S. (2001). Measurement of Radioactivity and Radon Exhalation Rate in Different Kinds of Marbles and Granites. *Appl. Radiat. Isot*. 55, 853–860.

[27] Righi, S., Guerra, R., Jeyapandian, M., Verita`, S. and Albertazzi, A. (2009). Natural Radioactivity in Italian Ceramic Tiles. *Radioprotection* 44(5), 413–419.

[28] EC. (1999). European Commission Report on Radiological Protection Principles Concerning the Natural Radioactivity of Building Materials. *Radiation Protection* 112.

[29] Beretka, J. and Mathew, P. J. (1985). Natural Radioactivity of Australian Building Materials, Industrial Wastes and by Products. Health Phys. 48(1), 87–95.

[30] Erkan, A. (2007). An Investigation on The Natural Radioactivity of Building Materials, Raw Materials and Interior Coatings in Central Turkey. Turkey *J. Med. Sci.* 37(4), 199–203.

[31] UNSCEAR (1993). (United Nations Scientific Committee on the Effects of Atomic Radiation). Exposure from Natural Sources of Radiation of Radiation. *Report to the General Assembly*. 549-552.

[32] Farai, I. P. and Ejeh, J. E. (2006). Radioactivity Concentrations in Common Brands of Cement in Nigeria. *Radioprotection* 41(4), 455–462.

[33] Malanca, A., Pessina, V. and Dallara, G. (1993). Radionuclide Content of Building Materials and Gamma Ray Dose Rates in Dwellings of Riograndе do Norte Brazil. *Radiat. Prot. Dosim.* 48(2), 199–203.

[34] Al-Saleh, F. S. and Al-Berzan, B. (2007). Measurements of Natural Radioactivity in Some Kinds of Marble and Granite Used in Riyadh Region. *J. Nucl. Radiat. Phys*. 2(1), 25–36.

[35] Anjos, R. M., Juri, A. J., Cid, A. S., Cardoso, R. and Lacerda, T. (2011). External Gamma-Ray Dose Rate and Radon Concentration in Indoor Environments Covered with Brazilian Granites. *J Environ. Radioact*. 102, 1055–1061.

[36] Mustapha, A. O., Pater, J. P. and Rathore, I. V. S. (1999). Assessment of Human Exposures to Natural Sources of Radiation in KENYA. *Radiat. Prot. Dosim.* 82(4), 285–292.

[37] UNSCEAR (1988). (United Nations Scientific Committee on the Effects of Atomic Radiation). Sources and effects of Ionizing Radiation, United Nation press, 641-643.

[38] Lee, S. C., Kim, C. K., Lee, D. M. and Kang, H. D. (2001). Natural Raaionuclides Contents and Radon Exhalation Rates in Building Materials Used in South Korea. *Radiat. Prot. Dosim.* 94(3), 269–274.

[39] Mustonen, R. (1984). Methods of Evaluation of Radiation from Building Materials. *Radiat. Prot. Dosim*. 7(7), 235–238.

[40] Koblinger, L. (1984). Mathematical Models of External Gamma Radiation and Congruence of Measurements. *Radiat. Prot. Dosim*. 7(7), 227–234.

[41] Risica, S., Bolzan, C. and Nuccetelli, C. (2001). Radioactivity in Building Materials: Room Model Analysis and Experimental Methods. *Sci. Total Environ*. 272, 119–126.

[42] Markkanen, M. (1995). Radiation Dose Assessments for Materials With Elevated Natural Radioactivity. *Radiation and Nuclear Safety Authority STUK*. Report B-STO 32.

[43] Abbasi, A. (2013). Calculation of Gamma Radiation Dose Rate and Radon Concentration Due to Granites Used As Building Materials in Iran. *Radiat. Prot. Dosim*. 155(3), 335-342.

[44] IAEA. (1998). Measurement of Radionuclides in Food and Environmental Samples. International Atomic Energy Agency. *IAEA Technical Report* 295.

[45] Mustonen, R. (1984). Natural Radioactivity In and Radon Exhalation from Finnish Building Materials. *Health Phys.* 46, 1195–1203.

[46] Stranden, E. (1976). Some Aspects on Radioactivity of Building Materials. *Phys. Norv*. 8, 167–173.

[47] Allen, J. G., Minegishi, T., Myatt, T. A., Stewart, J. H., Mccarthy, J. F. and Macintosh, D. L. (2010). Assessing Exposure to Granite Countertops-Part 2: Radon. *J. Exposure Sci. Environ. Epidemiol*. 20, 263–272.

[48] Chen, J., Rahman, N. M. and Atiya, I. A. (2010). Radon Exhalation from Building Materials for Decorative Use. *J. Environ. Radioact*. 101, 317–322.

[49] ICRP (2006). Draft Recommendations of the International Commission on Radiological Protection. *International Commission on Radiological Protection*.

[50] Nassiri, P., Ebrahimi, H. and Jafari Shalkouhi, P. (2011). Evaluation of Radon Exhalation Rate From Granite Stone. *J. Sci. Ind. Res*. 70, 230–231.

[51] Chao, C. Y. H. and Tung, T. C. W. (1999). Radon Emanation of Building Material—Impact of Back Diffusion and Difference Between One-Dimensional and Three-Dimensional Tests. *Health Phys.* 76, 675–681.

[52] Arafa,W. (2004). Specific Activity And Hazards of Granite Samples Collected from The Eastern Desert of Egypt. *J. Environ. Radioact*. 75, 315–327.

[53] Kitto, M. and Green, J. (2005). Emanation from Granite Countertops. In: *Proceedings of International Radon Symposium,* San Diego, UAS.152-153.

[54] Xinwei, L., Lingqing, W. and Xiaodan, J. (2006). Radiometric Analysis of Chinese Commercial Granites. *J. Radioanal. Nucl. Chem*. 267(3), 669–673.

[55] Stoulos, S., Manolopoulou, M. and Papastefanou, C. (2003). Assessment of Natural Radiation Exposure and Radon Exhalation from Building Materials in Greece. *J. Environ. Radioact.* 69, 225–240.

[56] Gillmore, G. K. and Jabarivasal, N. (2010). Reconnaissance Study of Radon Concentrations in Hamadan City Of Iran. *Nat. Hazards Earth Syst*. Sci. 10, 857–863.